

Photoelectrochemical reactors for CO₂ utilization

Sergio Castro^{*}, Jonathan Albo and Angel Irabien

Department of Chemical & Biomolecular Engineering, University of Cantabria, Avda. Los Castros s/n,
39005 Santander, Spain

^{*}Corresponding author, email: sergio.castro@unican.es

ABSTRACT

The photoelectrochemical reduction of CO₂ to renewable fuels and valuable chemicals using solar energy is a research topic that has attracted great attention recently due to its potential to provide value added products under the sun, solving the issues related to global warming at the same time. This review covers the main research efforts made on the photoelectrochemical reduction of CO₂. Particularly, the study focuses in the configuration of the applied reactor, which is a topic scarcely explored in the literature. This includes the main materials used as photoelectrodes and their configuration in the photoelectrochemical reactor, which are discussed for technical uses. The review provides an overview of the state-of-the-art and aims to help in the development of enhanced photoelectroreactors for an efficient CO₂ utilization.

KEYWORDS: Photoelectrocatalysis; CO₂ reduction; reactor configurations; photoelectrodes; climate change

INTRODUCTION

The reduction of fossil fuels and the growing emission of carbon dioxide (CO₂) have accelerated research activities to produce fuels and chemicals from wasted CO₂ as a

1
2
3 carbon source. CO₂ can be considered an unlimited, renewable and valuable carbon
4
5 source instead of a greenhouse gas emission. However, due to the chemical properties of
6
7 CO₂, its transformation requires a high level of energy since the bond dissociation energy
8
9 of C=O is ~750 kJ·mol⁻¹, higher than other chemical bonds such as C-H (~430 kJ·mol⁻¹)
10
11 and C-C (~336 kJ·mol⁻¹).¹ Nowadays, there are several technologies able to chemically
12
13 reduce CO₂ to value added products. Among them: thermochemical processes (i.e.
14
15 hydrogenation, reforming), mineralization, electrochemical reduction and
16
17 photo/photoelectro-chemical reduction.² Compared to thermochemical processes,
18
19 mineralization processes present limitations that should be solved through further
20
21 technological developments due to the low carbonation rates, high cost and energy
22
23 penalties. It is also possible to dissociate CO₂ and H₂O by thermolysis at extremely high
24
25 temperatures. Electrochemical processes, however, permit to dissociate H₂O or CO₂ at
26
27 ambient conditions using electricity and has attracted worldwide interest due to their
28
29 potential environmental and economic benefits.³ This technology not only offer a viable
30
31 route to reuse CO₂ but also an excellent alternative to store intermittent energy from
32
33 renewable sources in the form of chemical bonds.^{4, 5} When electrochemical reduction
34
35 integrates a light source, a photoelectrochemical device is obtained, which has attracted
36
37 an intense progress in recent years.^{6, 7} In principle, such integration reduces the system
38
39 capital cost and enables higher efficiency by reducing losses in transporting electricity to
40
41 the electrolysis cell, eliminating current collectors and interconnections between devices.
42
43 The operation of a photoelectrochemical (PEC) cell is inspired by natural photosynthesis
44
45 in which carbohydrates are formed from CO₂. The goal is to use excited electrons that are
46
47 generated when the semiconductor absorbs light to effect electrochemistry on a redox
48
49 couple strategically chosen to produce the desired chemicals.⁸
50
51
52
53
54
55
56
57
58
59
60

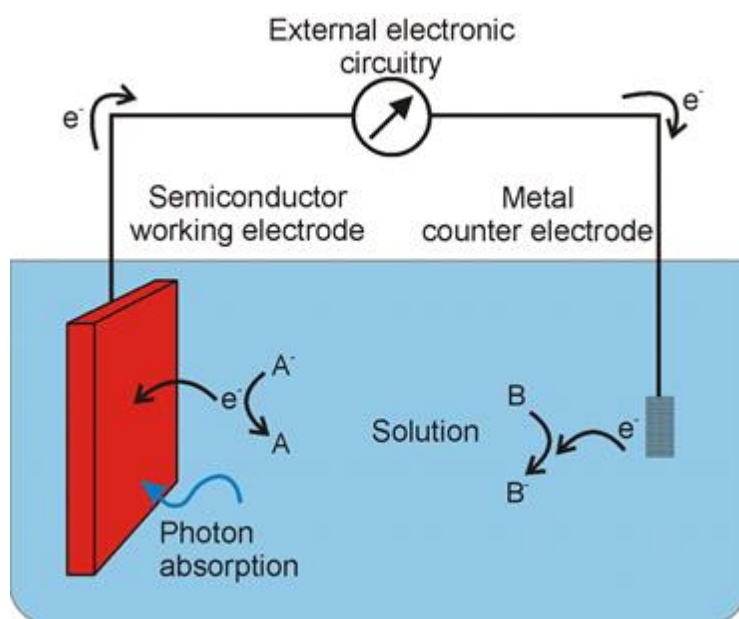


Figure 1. Photoelectrochemical setup.⁹

The concept of a photoelectrochemical cell is comparable to a conventional electrochemical cell, except that energy necessary to cause redox reactions is partially provide by the light. This concept is represented in Figure 1. A semiconductor material absorbs the light at the working electrode, exciting electrons to a higher energy level that, together with the corresponding holes generated, are able of carrying out reduction and oxidation reactions at a semiconductor/liquid interface. In practice, several characteristics of the photoelectrodes must be satisfied simultaneously: the electronic band gap of the photoelectrode must be low enough for efficient photon collecting from the solar spectrum (<2.2 eV) and high enough such that the excited electrons have enough energy to split water (>1.23 eV or typically at least 1.6 – 1.7 eV for sufficient rates), the band edges must cover the water electrolysis redox potentials and the photoelectrode must be stable and resistant to corrosion in the aqueous electrolyte.¹⁰ The photoelectrochemistry is therefore a thrilling and interdisciplinary research fied that includes electrochemistry, surface science, solid-state physics and optics.¹¹

1
2
3 CO₂ can be converted to a wide range of products such as CO, H₂, HCOOH, CH₃OH,
4
5 CH₄, etc.¹² Equations 1–5 shows the thermodynamic potentials for CO₂ reduction
6
7 products at neutral pH in aqueous solution versus a saturated calomel electrode (SCE)
8
9 and 25°C and atmospheric pressure: ¹³



31
32
33
34
35 The extent to which the reaction progresses depends mainly on the catalytic systems, as
36
37 well as the reaction media and potential applied.¹² Typically, multiple proton coupled
38
39 electron transfer steps must be orchestrated, presenting kinetic barriers to the forward
40
41 reaction.¹³ Besides, part of the energy supplied to the system may be consumed by the
42
43 competitive reaction for H₂ production from water electrolysis in the Hydrogen Evolution
44
45 Reaction (HER). The state-of-the-art for the production of value added products from
46
47 CO₂ using solar energy is still far from practical consideration, but knowledge has been
48
49 accumulated through the years.¹⁴ Since the first report in 1978 on CO₂
50
51 photoelectrochemical reduction by Halman,¹⁵ many review articles have been writing
52
53 about different aspects of this photoelectrochemical technology, as shown in Table 1. In
54
55 2014, Ibrahim et al.⁹ collected the available knowledge about photoelectrochemical
56
57
58
59
60

1
2
3 reactions to produce biofuel from biomass. In 2015, Sudha et al.¹⁶ review the recent
4
5 developments in the synthesis and application of composite photocatalysts derived from
6
7 TiO₂, CdS, WO₃, SnS and ZnO. Moreover, Nikokavoura et al.¹⁷ presented alternative
8
9 photocatalysts to TiO₂ for the photoelectroreduction of CO₂. Inorganic and carbon based
10
11 semiconductors, mixed-metal oxides, salt composites and other groups of photocatalyst
12
13 were examined in this review. Moreover, a simplified energetic and economic feasibility
14
15 assessment for a solar refinery (including photoelectrochemical means) for the production
16
17 of methanol was developed by Herron et al.^{18, 19}, concluding that at least a 15% solar-
18
19 to-fuel efficiency is required in order to compete with industrial methanol production.
20
21 Besides, one of the most important factors affecting the CO₂ reduction performance is the
22
23 configuration of the photoreactor. A complete discussion on photoreactor analysis
24
25 and design was carry out by P.L. Yue in 1985.²⁰ In this paper, the author presented and
26
27 overview of the important engineering problems in the modelling and design of
28
29 photoreactors. More recently, Cassano et al.²¹ in 2005, described the most important
30
31 technical tools that are needed to design photoreactors using computer simulation of a
32
33 rigorous mathematical description of the reactor performance, both in the laboratory and
34
35 on a commercial scale.
36
37
38
39
40
41
42
43
44

45 Table 1. List of review articles on CO₂ photoelectrochemical reduction.

46 Author (year)	47 Publication title	48 Ref.
49 A. J. Bard (1979)	50 Photoelectrochemistry and heterogeneous photo- 51 catalysis at semiconductors	22
52 D.A. Tryk (2000)	53 Recent topics in photoelectrochemistry: 54 achievements and future prospects	23
55 B. Kumar (2012)	56 Photochemical and Photoelectrochemical 57 Reduction of CO ₂	13
58 A. Harriman (2013)	59 Prospects for conversion of solar energy into 60 chemical fuels: the concept of a solar fuels industry	7

S. N. Habisreutinger (2013)	Photocatalytic reduction of CO ₂ on TiO ₂ and other semiconductors	24
N. Ibrahim (2014)	Biofuel from biomass via photo-electrochemical reactions: An overview	9
J. Zhao (2014)	Hybrid catalysts for photoelectrochemical reduction of carbon dioxide: a prospective review on semiconductor/metal complex co-catalyst systems	25
J. Highfield (2015)	Advances and Recent Trends in Heterogeneous Photo(Electro)-Catalysis for Solar Fuels and Chemicals	26
Y. Yan (2015)	Photoelectrocatalytic Reduction of Carbon Dioxide	8
C. Ampelli (2015)	Electrolyte-less design of PEC cells for solar fuels: Prospects and open issues in the development of cells and related catalytic electrodes	27
D. Sudha (2015)	Review on the photocatalytic activity of various composite catalysts	16
S. Xie (2016)	Photocatalytic and photoelectrocatalytic reduction of CO ₂ using heterogeneous catalysts with controlled nanostructures	28
A. Nikokavoura (2017)	Alternative photocatalysts to TiO ₂ for the photocatalytic reduction of CO ₂	17
L. Y. Ozer (2017)	Inorganic semiconductors-graphene composites in photo(electro)catalysis: Synthetic strategies, interaction mechanisms and applications	29
P. Wang (2018)	Recent Progress on Photo-Electrocatalytic Reduction of Carbon Dioxide	30

In any case, it seems that the effect of reactor configuration in the CO₂ photoreduction performance has not been discussed in literature as much as the development of active materials. To fill this gap, the aim of the present review is to provide a deeper analysis on the photoelectroreduction of CO₂ in terms of photoelectrochemical cell and photoelectrodes configuration, together with a discussion on photoactive materials applied and obtained products for each configuration as key variables in process performance. The discussion is structured as follows: (i) Photoelectrochemical reactor

1
2
3 configurations, (ii) Photoelectrode materials, (iii) Main reduction products and finally,
4
5 (iv) Conclusions and future challenges. This compilation aims to be a step further towards
6
7 real application of photoelectroreactors for CO₂ conversion.
8
9

10 11 12 **SUMMARY OF STUDIES**

13 14 15 **PEC reactor configuration**

16
17
18 The reactor can be considered the heart of a photoelectrochemical system. In a PEC
19
20 reactor, the illumination of the photoactive surface becomes crucial, together with other
21
22 common variables in reactors such as mass transfer, mixing or reaction kinetics.³¹ The
23
24 design should be made based on a careful evaluation of different factors influencing
25
26 reaction performance:^{20, 21} (i) light source and geometrical configuration, (ii)
27
28 construction material, (iii) heat exchange, (iv) mixing and flow characteristics and (v)
29
30 phases involved and mode of operation.³² These are discussed as follows:
31
32
33
34
35

36
37 (i) For optimum results, light needs to be distributed homogeneously through the entire
38
39 photoactive surface.³³ The choice of the most suitable light source can be made by
40
41 evaluating the reaction energy requirements with respect to the lamp specifications. The
42
43 well-known Xenon arc lamp seems to be the most employed lamp in literature. This lamp
44
45 produces a bright white light that closely mimics natural sunlight when electricity pass
46
47 through the ionized Xe gas at high pressure.^{34, 35} If solar energy is being considered, it
48
49 should be noticed that sunlight mainly consists of three different wavelengths: ultraviolet
50
51 ($\lambda < 400$ nm), visible ($\lambda = 400-800$ nm) and infrared ($\lambda > 800$ nm), accounting for 4%,
52
53 53%, and 43% of the total solar energy, respectively.³⁶ Moreover, it is recommended to
54
55 give a certain pattern of irradiation by mounting the light source inside a glass sheath or
56
57 some suitable optical assembly as Ampelli et al.³⁷ evaluated where the Xe-arc lamp of
58
59
60

1
2
3 300 W was protected by a housing and a set of lenses were employed. Regarding
4 geometrical configuration, it is necessary to determine the optical path of the light inside
5 the reactor, in a way to obtain the maximum benefit from the irradiation pattern and a
6 good absorption of light photons. For photo-reactors, other aspects such as the spatial
7 relation between reactor and light source and geometry are crucial. In all cases, the
8 irradiation takes place normal to the reactor surface.
9

10
11
12
13
14
15
16
17
18
19 (ii) In photo-reactors, the requirements of light transmission influenced in the
20 construction material election. The choice is usually limited to different types of glass
21 being the Pyrex glass the most used in the bibliography for its adequate light transmission
22 and cost,³⁸⁻⁴⁰ although quartz glass is more expensive, but generally gives the best
23 performance in terms of light transmission. At short wavelengths ($\lambda < 300$ nm) quartz
24 seems to be the only appropriate material. In some cases, the glass has been substituted
25 by the plastic Plexiglas, except the reactor window, which continuous being made of glass
26 to allow UV light transmittance. For instance, Cheng et al.⁴¹ reduced CO₂ using a PEC
27 Plexiglas reactor with a quartz window achieving a light intensity at the anode surface of
28 10 mW·cm⁻² with a 300 W Xe-arc lamp. Another important factor is the thickness of the
29 reactor wall, which decreases the light transmission and limited the size of the reactor and
30 the operating temperature and pressure. Others authors,^{42, 43} use a different design to
31 illuminate the photocatalyst surface, avoiding the problems of construction materials and
32 light transmission by combining the PEC cell with a solar panel (PEC-photosolar cell
33 tandem). Thus, the photomaterial is directly illuminated, the light is not disturbed by
34 aqueous media and H₂O could be oxidized in the photoanode without applying external
35 bias.
36
37
38
39
40
41
42
43
44
45
46
47
48
49
50
51
52
53
54
55
56
57
58
59
60

(iii) Heat exchange should be particularly considered, especially in gas-solid systems. Suitable devices must be designed to remove the heat generated by the lamp, because of the glass low thermal conductivity.³² For example, Ong et al.⁴⁴ positioned a water jacket between the PEC cell systems and the Xe arc lamp to lessen the effects of heat on the Na₂SO₄ electrolyte solution during irradiation.

(iv) Mixing and flows depend on the phases involved in the process are also important factors to take into account. It is recommended to mix. In the case of heterogeneous photo-reactions, contact between reactants, photons and catalysts should be promoted, for example with agitation of the reacting mixture using a stirrer.³²

(v) Photoreactors applied for CO₂ photoconversion can be classified according to the phases involved (i.e., gas-solid, liquid-solid, gas-liquid-solid, etc.) and the mode of operation (i.e., batch, semi-batch or continuous). Moreover, the materials can be generally in suspended (fluidized bed) or immobilized forms (fixed bed) in reactors. The main pros and cons of different current photoreactor systems for CO₂ transformation are summarized in Table 2.³³ Figure 2 shows the schematic configuration of various types of photocatalytic reactors, which may serve as a reference for the design of new photoelectrocatalytic reactors (i.e. light incidence, flows inlet/outlet, photoactive surface configuration, etc.).

Table 2. Photoreactor systems: advantages and disadvantages.

Reactor design	Advantages	Disadvantages	Ref.
Fluidized and slurry reactor	-Temperature gradients inside the beds can be reduce	-Filters (liquid phase) and scrubbers (gas) are needed.	45-47

(multiphase)	<p>through vigorous movements caused by the solid passing through the fluids.</p> <p>-Heat and mass transfer increase due to agitated movement of solid particles.</p> <p>-High catalyst loading.</p>	<p>-Flooding tends to reduce the effectiveness of the catalyst.</p> <p>-Difficulty of separating the catalyst from the reaction mixture.</p> <p>-Low light utilization efficiency due to absorption and scattering of the light by the reaction medium.</p> <p>-Restricted processing capacities due to limitations in mass transfer.</p>	
Fixed bed reactor	<p>-High surface area.</p> <p>-Fast reaction time.</p> <p>-The conversion rate per unit mass of the catalyst is high due to the flow regime close to plug flow.</p> <p>-Low operating cost due to a reduced pressure drop.</p>	<p>-Temperature gradient between gas and solid surface.</p>	48, 49

Monolith reactor	<ul style="list-style-type: none">-High surface to volume ratio and low pressure drop with high flow rate.-Configuration can be easily modified.	<ul style="list-style-type: none">-Low light efficiency due to opacity of channels of the monolith.	50, 51
Optical fiber reactor	<ul style="list-style-type: none">-High surface area and light utilization efficiency.-Efficient processing capacities of the catalyst.	<ul style="list-style-type: none">-Maximum use of the reactor volume is not achieved.-Heat build-up of fibers can lead to rapid catalyst deactivation.	51, 52

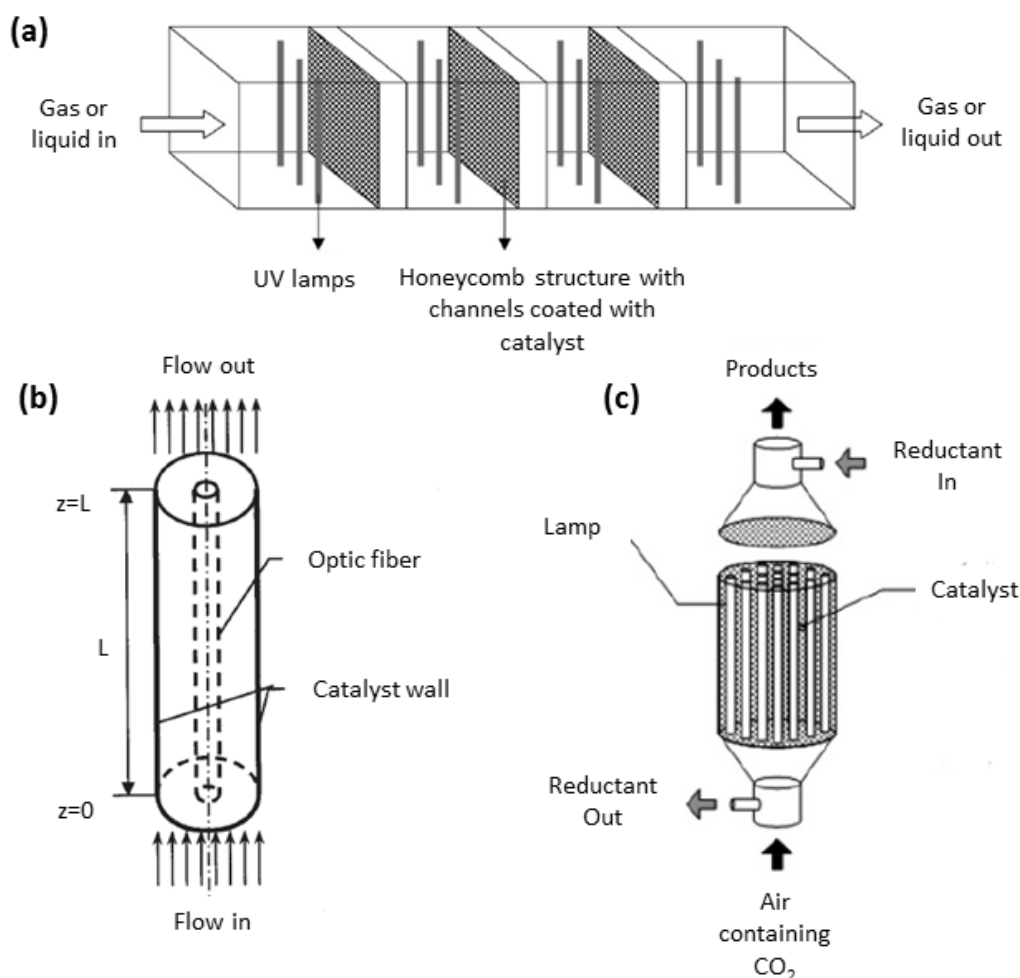


Figure 2. (a) Monolith photoreactor,⁵⁰ (b) Optical fiber photoreactor⁵¹ and (c) Fixed bed photoreactor.⁴⁵

The recirculation of unconverted CO₂ also must be taken into account when designing an effective photoelectroreactor, since the separation of the products from CO₂ could account for 6-17% of the total energy required in the process.⁵³ Moreover, undivided photoelectrochemical reactors (Figure 3), in which plate-type electrodes are separated by a liquid phase that acts as both anolyte and catholyte have been commonly used. In these type of cells, the process costs increase due to the extra separation step required for the product recuperation.⁵⁴ For a practical use of PEC cells, the separation in two distinct

1
2
3 compartments where CO₂ reduction and water oxidation take place, is more appealing
4 than the single compartment process, since one can deal with one reaction at a time. As a
5
6 result, the efficiency of the redox reactions increase, as so the charge recombination and
7
8 products separation .^{37, 55, 56} The election between single and dual compartment cell does
9
10 not follow a determinant rule and depends on the case, although dual compartment cells
11
12 are usually preferred.^{37, 38, 40}

13
14
15 Besides, in order to allow an efficient collection/transport of electrons over the entire film
16
17 as well as the diffusion of protons through the membrane (Figure 4), both anode and
18
19 cathode should be in the form of a thin film separated by a proton-conducting membrane
20
21 (Nafion or other materials)^{37, 57} and fixed onto a porous conductive substrate in the PEC
22
23 cell. For CO₂ photoreduction, an efficient evolution of oxygen on the anode side is also
24
25 needed, together with an efficient evolution of CO₂ and diffusion of reaction products on
26
27 the cathode side. Moreover, the use of gas diffusion electrodes (GDEs) and gas phase
28
29 operation on the cathode compartment is preferable, in order to avoid the limitations of
30
31 CO₂ solubility.^{37, 58}

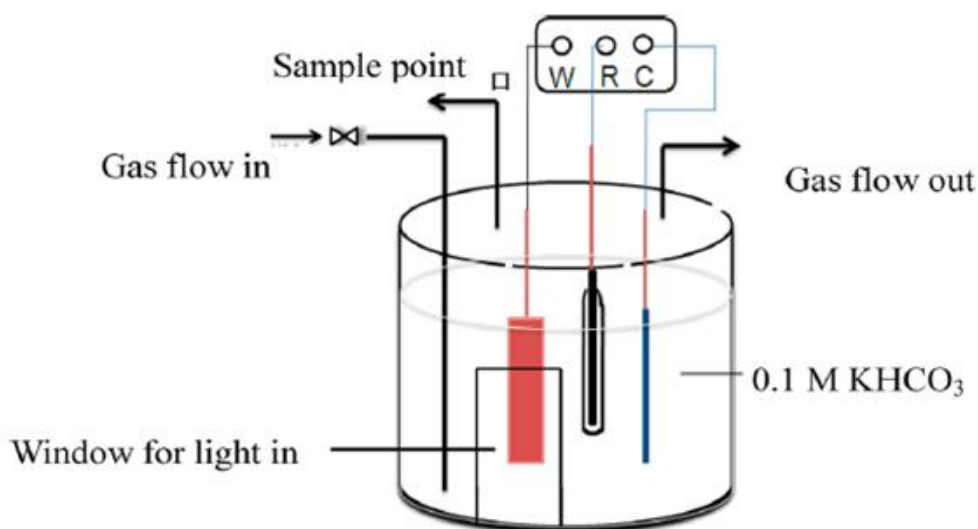


Figure 3. Single compartment cell (W= working electrode, R= reference electrode, and C=counter electrode).⁵⁹

The mass transport in the electrode is a limiting factor as better catalyst are progressively becoming available. For this, several elements have been considered: high pressure operation, the use of GDEs and no aqueous electrolytes.⁶⁰ GDEs usually consists of a carbon fiber substrate (CFS), a micro porous layer (MPL), typically is composed of carbon powder and polytetrafluoroethylene (PTFE), and a catalyst layer (CL). Del Castillo et al.,⁶¹ compared a Sn-GDE with a Sn plate electrode and obtained higher rates for the Sn-GDE than for Sn plate electrode, demonstrating the exceptional performance of GDEs for CO₂ reduction.^{60, 62} Gas phase CO₂ transformation by using GDEs can be also applied to enhance CO₂ transfer, allowing the operation at higher current densities in the cell as demonstrated by Merino-Garcia et al.,⁶³ in a dual compartment cell for methane and ethylene production by using a Cu-based membrane electrode assembly (MEA).

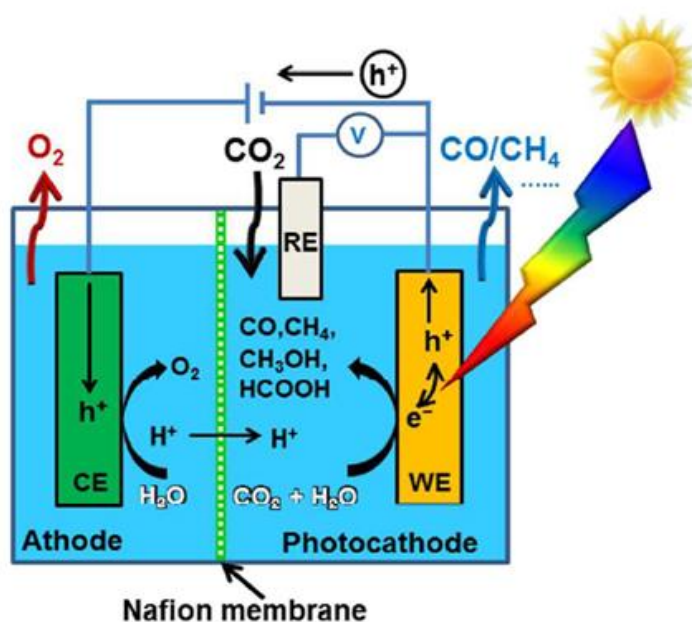


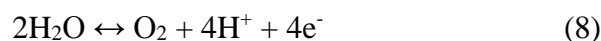
Figure 4. Dual compartment cell.⁶⁴

Moreover, the type of ion transport membrane applied is key in the CO₂ photoelectrochemical reduction performance, where proton exchange membranes (PEMs) are preferred due to their favored protons transport from the anode to the cathode than the anion exchange membranes (AEMs), with anions transported from the cathode to the anode compartment, but of course it may depend on the reaction conditions and cell configuration.⁵⁴ The expected reactions in a PEM-based reactors are:⁵⁵

Cathode:

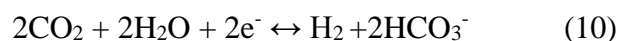


Anode:

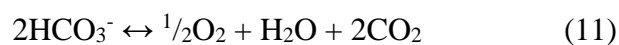


While the expected reactions in a AEM are:⁵⁵

Cathode:



Anode:



There are many examples on the use of PEMs in photoelectroreduction,^{5, 65, 66} while AEMs are not usually employed, although some examples are reported in electrochemical devices where current densities as high as 130 mA·cm⁻² can be achieved.⁶⁷ This is the case for the new anion-conductive polystyrene methyl methylimidazolium chloride (tradenamed SustainionTM) AEM membrane developed by Masel and co-workers, which

1
2
3
4
5
6
7
8
9
10
11
12
13
14
15
16
17
18
19
20
21
22
23
24
25
26
27
28
29
30
31
32
33
34
35
36
37
38
39
40
41
42
43
44
45
46
47
48
49
50
51
52
53
54
55
56
57
58
59
60

exceeded standards for product selectivity and current density with commercially available AEM.⁶⁷

Moreover, bipolar membranes (BPM), made of an anion and cation exchange membranes, have recently gain interest for CO₂ transformation due to their ability to separate anode and cathode compartments and the high sensitivity on pH required to facilitate different electrolyte conditions for the anode and for the cathode by the selective transport of OH⁻ to the anode and H⁺ to the cathode.^{68,69} Maintaining the pH constant, BPMs allow the use of new earth-abundant metal anodes that are stable in basic conditions and highly active acid-stable cathodes for CO₂ reduction, which cannot be realized by using PEMs and AEMs.⁶² Recently, Zhou et al.,⁶⁹ reported a FE >94% to HCOOH (8.5 mA·cm⁻²) using a GaAs/InGaP/TiO₂/Ni photoanode and a Pd/C nanoparticle-coated Ti mesh cathode, employing as electrolytes 1.0 M KOH (pH=13.7) and 2.8 M KHCO₃ (aq) (pH=8.0) separated by a BPM that facilitated the separation of redox reactions to achieve higher efficiencies and produce lower total overpotentials in comparison to a single compartment cell.

In addition, the formation of liquid products from CO₂ reduction has mostly focused on batch PEC reactors.^{3,4,70,71} Only a few researchers deal with the concept of continuous flow photoelectrochemical reactors,⁷² required in the production at industrial scale, minimizing capital costs and maximizing product consistency as demonstrated in case of electrochemical systems for CO₂ continuous reduction. To this end, a continuous flow PEC reactor (CFPR) was developed in 2015 by Homayoni et al.⁷³ to produce alcohols from CO₂ employing a CuO/Cu₂O photocathode (Figure 5). The results show long-chain alcohol products up to C₂-C₃ (ethanol and isopropanol) with a production rate of 0.22 ml·m⁻²·h⁻¹, that was approximately 6 times higher than in a batch design.

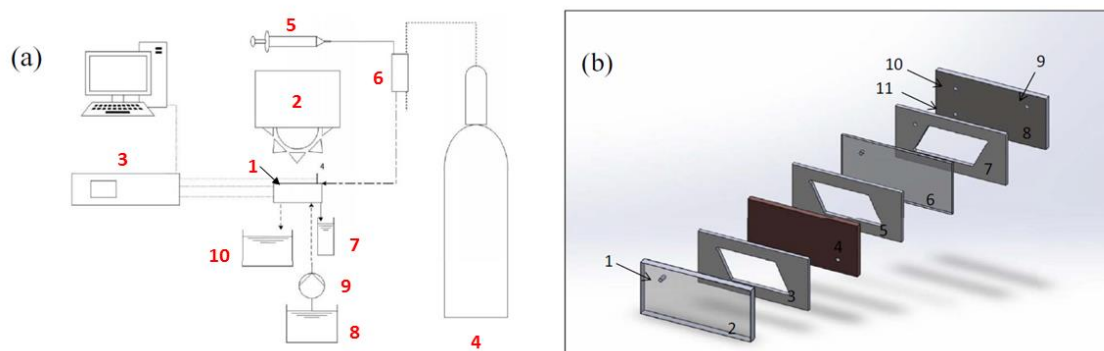


Figure 5. (a) Schematic diagram of the CFPR set-up: (1) CFPR, (2) solar simulator, (3) electrochemical workstation, (4) CO₂ tank, (5) syringe pump, (6) fresh catholyte from a gas mixing chamber, (7) catholyte collector, (8) fresh anolyte, (9) pump, and (10) anolyte collector. The electrical connections to the electrodes are marked as WE, CE and RE for the cathode, anode and reference electrode respectively. (b) Schematic diagram of the CFPR itself consisting of: (1) catholyte inlet and location of the reference electrode, (2) optical window (transparent slab), (3) microchannel arrays slab on top of the cathode, (4) cathode, (5) microchannel arrays underneath the cathode, (6) ion exchange membrane, (7) microchannel arrays on top of the anode, (8) anode, (9) outlet of anolyte, (10) outlet of catholyte, and (11) inlet of anolyte.⁷³

Furthermore, there are different electrode configurations for the PEC systems on dependence on which electrode (i.e., anode, cathode, or both) acts as photoelectrode,⁶⁵ as described in the following subsections.

Photocathode-dark anode.

Most of the studies employed a photocathode made of a *p*-type semiconductor, with a high conduction band energy suitable for CO₂ reduction, and an anode made of metal (Figure 6).^{74, 75} The first study was reported by Halmann in 1978, where a *p*-GaP semiconductor was used as photocathode, carbon rod as counter electrode and a buffered

aqueous solution as electrolyte.¹⁵ A $6 \text{ mA}\cdot\text{cm}^{-2}$ current was detected when *p*-GaP was illuminated with an Hg lamp and a voltage bias of -1 V vs. SCE was applied. HCOOH, HCHO and CH₃OH were formed. More recently, this type of configuration was implemented by Qin et al.⁷⁶ using TiO₂ as photocathode and an electrode of Pt as anode to obtain HCOOH, HCHO and CH₃OH as main products.

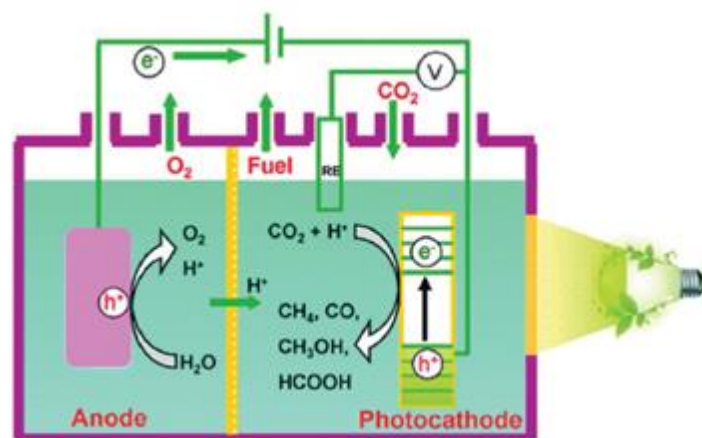


Figure 6. Semiconductor as photocathode.²⁸

Unfortunately, the valence band in *p*-type semiconductors does not cover H₂O oxidation and a bias potential is required. Besides, these materials are usually expensive, toxic and unstable and two-electron compounds, such as CO and HCOOH, are usually obtained as it was demonstrated by Kaneco et al.⁷⁷ when a metal-doped (Pb, Ag, Au, Pd, Cu and Ni) *p*-InP photocathode and a Pt foil as counter electrode was applied at -2.5 V vs. SCE (-2.5 V vs. Ag/AgCl) potential. Overall, the efficiency of *p*-type semiconductor-based systems is low, and the improvement required in photocathode efficiency remains a challenge.

Photoanode-dark cathode.

The use of a *n*-type semiconductor (e.g., TiO₂, ZnO, BiVO₄ or WO₃) which are earth-abundant, cheap and stable as photoanode for H₂O oxidation, and a metallic electrocatalyst active for CO₂ reduction as the cathode to assemble a photoanode-dark

1
2
3 cathode PEC reactor is also an attractive option (Figure 7).^{41, 78} CO₂ reduction in a
4
5 photoanode-dark cathode PEC depends on two components: cathode catalysts and
6
7 photoanode activity. This cell could improve CO₂ reduction values obtained in
8
9 electrocatalytic systems and reduce energy input over the photoanode catalyst, requiring
10
11 a lower external bias for an effective CO₂ reduction than the photocathode-dark anode
12
13 configuration.^{28, 65} In this configuration, the photoanode plays a dual role during CO₂
14
15 reduction. On the one hand, the voltage generated by the light in the anode supply an extra
16
17 negative potential to the cathode for CO₂ reduction and on the other hand, protons and
18
19 electrons for CO₂ reduction in the cathode were provided by the oxidation of water in the
20
21 anode.⁶⁵ Chang and coworkers⁷⁹ used TiO₂ as a model photoanode and Cu₂O as a dark
22
23 cathode to devise a stable system for photoconversion with a FE of 87.4% and a
24
25 selectivity of 92.6% for carbonaceous products from CO₂. For instance, a Pt-modified
26
27 reduced graphene oxide (Pt-RGO) cathode and a Pt modified TiO₂ nanotubes (Pt-TNT)
28
29 photoanode converted CO₂ into HCOOH, CH₃OH, CH₃COOH and C₂H₅OH under UV-
30
31 Vis irradiation, applying a potential of 2 V.⁴¹ In further investigations, the cathode was
32
33 substituted by Pt-RGO/Cu foam⁷⁸ and Pt-RGO/Ni foam⁶⁵ to improve products
34
35 selectivity.
36
37
38
39
40
41

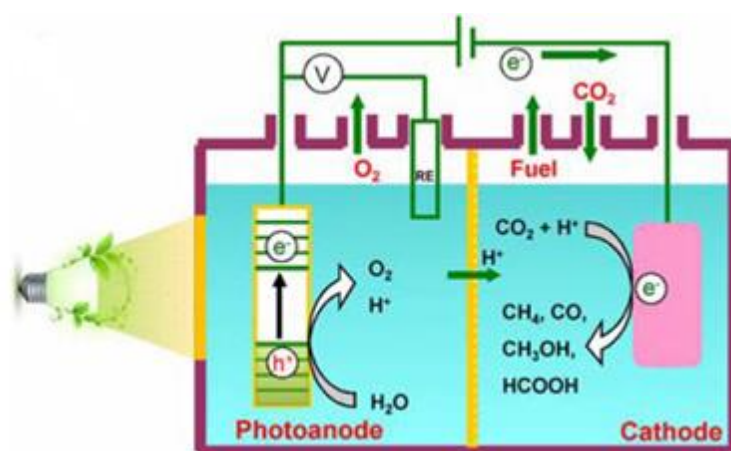


Figure 7. Semiconductor as photoanode.²⁸

Photocathode-photoanode.

Another option for the photoelectrodes in an assembly of PECs is the combination of a photocathode made of a *p*-type semiconductor for CO₂ reduction with a photoanode made of a *n*-type semiconductor for H₂O oxidation (Figure 8). This configuration, in contrast to the other two, allow realizing the transformation of CO₂ with H₂O without external electrical energy. In this case, the conduction band edge of the photoanode for H₂O oxidation must be more negative than the valence band edge of the photocathode for CO₂ reduction to guarantee the electron transfer from photoanode to photocathode through the external wire.²⁸ Sato et al.³⁸ employed this PEC configuration to produce HCOOH in a two-compartment Pyrex cell separated by a PEM using InP/[MCE]s and TiO₂/Pt as photocathode and photoanode respectively. By applying a light source, the two-compartment PEC cell could be run without external applied electrical energy. Not all the photocathode and a photoanode PECs cell configuration reported in literature are able to reduce CO₂ without an external potential. Some need extra electrical energy to overcome parasitic losses and reaction overpotentials, such as *p*-type Si nanowire/*n*-type TiO₂ nanotube where traces of C₃–C₄ hydrocarbons, CH₄ and C₂H₄ were formed under band gap illumination and at 1.5 V vs. Ag/AgCl.⁸⁰

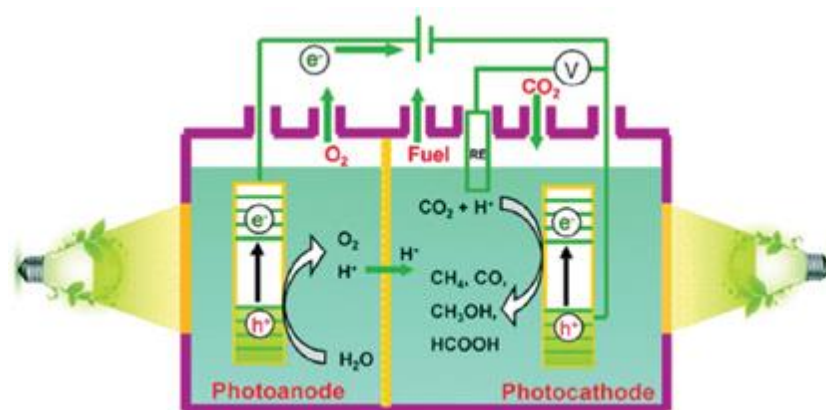


Figure 8. Semiconductors as both photocathode and photoanode.²⁸

PEC-solar cell tandem.

Traditionally, PEC cells and PV-electrolyzers are considered as different approaches, although some authors as Jacobsson et al.⁸¹ suggest that in many cases both approaches have certain similarities and should be considered under the acronym photo driven catalytic (PDC) devices. To be clear, a distinction should be made between the solar panel coupled in the photoanode⁴² (PEC-solar cell tandem, Figure 9), and the photovoltaic panels used as electric source to the PEC cell (PV-electrolyzers), which is the same as electroreduction using renewable energy.^{43, 82, 83} In order to value the potential importance that can develop the PEC-solar cell tandem configuration in photoelectroreduction, the authors consider treating this configuration as one more added to the previous.

The main benefit of using a PEC cell (i.e. photocathode-anode, cathode-photoanode, photocathode-photoanode or PEC-solar cell tandem) than PV-electrolyzers is the possibility to deal with the generation of electrons required and the oxidation of H₂O (if a photoanode is employed) or adjust the redox potential to the interest product (if a photocathode is used) in the same device.

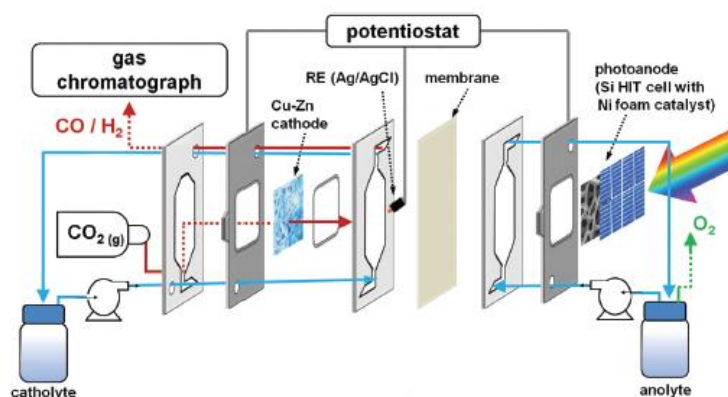


Figure 9. Filter-press reactor including a Cu-Zn cathode and a Si/Ni foam photoanode.⁴²

1
2
3 Figure 9 is an example of a PEC-solar cell tandem. An experimental set-up using Si
4 heterojunction solar cells in combination with Ni foam as photoanode and Zn coated Cu
5 foam as cathode was applied, reaching CO FEs up to 85% at 0.12 V vs. SCE (0.8 V vs.
6 RHE) with a CO current density of $39.4 \text{ mA}\cdot\text{cm}^{-2}$, the highest reported for a Zn catalyst
7 at such low overpotential. This reactor concept enhances the solar CO₂ conversion by the
8 use of the well-known and developed Si heterojunction technology, which is nontoxic,
9 abundant and cheap technology and it is being used in the photovoltaic industry
10 nowadays.⁴²
11
12
13
14
15
16
17
18
19
20
21
22

23 **Photoelectrode materials**

24
25
26 The next section briefly discusses on the main photoactive materials applied in the
27 different photoelectron-chemical reactor configurations for the reduction of CO₂.²⁴ The
28 two basic requirements for photoelectrode materials are optical response, to effectively
29 absorb sunlight, and catalytic activity, required for the CO₂ reduction and H₂O oxidation
30 reactions. In order to satisfy these requirements, the processing of materials with
31 enhanced performance characteristics need to include a high solar energy conversion
32 efficiency, stability in aquatic environments and low cost.⁹ In addition, the particle size
33 of the photoelectrode material has a considerable effect on CO₂ photoreduction efficiency
34 due to changes in CO₂ adsorption, available active surface area and transfer pathways for
35 charge carriers to reach its surface. The performance can be normally enhanced at smaller
36 particle sizes, although the smaller the size is the more the boundary of the particles,
37 which leads also to a lower activity. Furthermore, it has been proved that the best way to
38 improve the activity of photo-materials is controlling the facets of the photocatalysts
39 applied.⁸⁴
40
41
42
43
44
45
46
47
48
49
50
51
52
53
54
55
56
57
58
59
60

1
2
3 Typically, photoelectrocatalysis in contrast to common electrodes used in
4 electrocatalysis, employs semiconductor electrodes. In addition, graphene-based nano-
5 catalyst and organometallic complexes are commonly applied.² Semiconductor-based
6 electrodes absorb light to generate electron-hole pairs. The holes generated at the
7 photoanode, typically a *n*-type semiconductor, oxidize H₂O to O₂, while the electrons
8 photogenerated at the cathode, usually a *p*-type semiconductor, reduce the CO₂ to
9 valuable products such as CO, HCOOH, CH₃OH or hydrocarbons in the presence or
10 absence of a co-catalyst.²⁸ TiO₂, ZnO, CdS and SiC are the most employed inorganic
11 binary compounds as semiconductor materials.
12
13
14
15
16
17
18
19
20
21
22
23
24
25

26 *TiO₂ photoelectrodes*

27
28 TiO₂ is the most investigated semiconductor material for photocatalytic processes. It is a
29 *n*-type semiconductor that possesses a wide band gap (3.0 eV)⁸ and has been considered
30 a cheaper and more environmental friendly material since the first report in 1979.⁸⁵ TiO₂
31 has three kind of polycrystalline phases: anatase, brookite and rutile⁸⁶ with different
32 symmetries, slip directions, theoretical crystal densities, close stacking planes and
33 available interstitial positions, altering also the defect distribution and density. As an
34 example, Liu et al.⁸⁷ studied the photocatalytic reduction of CO₂ on three TiO₂
35 nanocrystal polymorphs pretreated with helium and concluded that for TiO₂ surfaces
36 engineered with defect sites, brookite provided the highest yield for CO and CH₄,
37 followed by anatase and rutile, probably due to a lower formation energy of oxygen
38 vacancies (V_O) on brookite.
39
40
41
42
43
44
45
46
47
48
49
50
51
52
53
54
55

56 The literature shows that TiO₂ has been tested for the photocatalytic reduction of CO₂
57 under various structures, such as nanosheets, nanocrystals, nanotube arrays, nanorods,
58
59
60

1
2
3 carbon-TiO₂ nanocomposites and mesoporous TiO₂-based materials.⁸⁸ Zhao et al.⁸⁹
4
5 reviewed the effects of surface point defects in the production of solar fuels from
6
7 CO₂ photoreduction in H₂O. In TiO₂, oxygen vacancies, impurities, Ti interstitials, Ti
8
9 vacancies, and defects at interfaces are examples of point defects. The defective
10
11 TiO₂ materials show superior performance than pristine TiO₂ for CO₂ photoreduction,
12
13 probably due to an enhanced dissociative adsorption of CO₂, an improved solar energy
14
15 absorption due to a change in the electronic band structure and a reduced charge
16
17 recombination due to the presence of charge traps. Unfortunately, TiO₂ mainly absorbs
18
19 UV radiation,⁹ which is only a small part of solar radiation. Although progresses have
20
21
22
23
24 been made with TiO₂, it seems that different materials should be considered in order to
25
26 enhance the photocatalytic transformation of CO₂ to useful products.
27
28
29

30 *Alternative photocatalyst to TiO₂*

31
32
33 Apart from TiO₂, other semiconductor-based photoelectrodes could be used. Figure 10
34
35 shows the band-gap positions of other semiconductor materials and the standard reduction
36
37 potentials for CO₂ reduction to different products. However, the photogenerated electrons
38
39 in the conduction band edge of all the candidate semiconductors do not have enough
40
41 driving force to carry out the activation of CO₂ to CO₂⁻ (-2.14 V vs. SCE), which defines
42
43 the efficiency for CO₂ photoreduction.⁶⁴
44
45
46
47
48
49
50
51
52
53
54
55
56
57
58
59
60

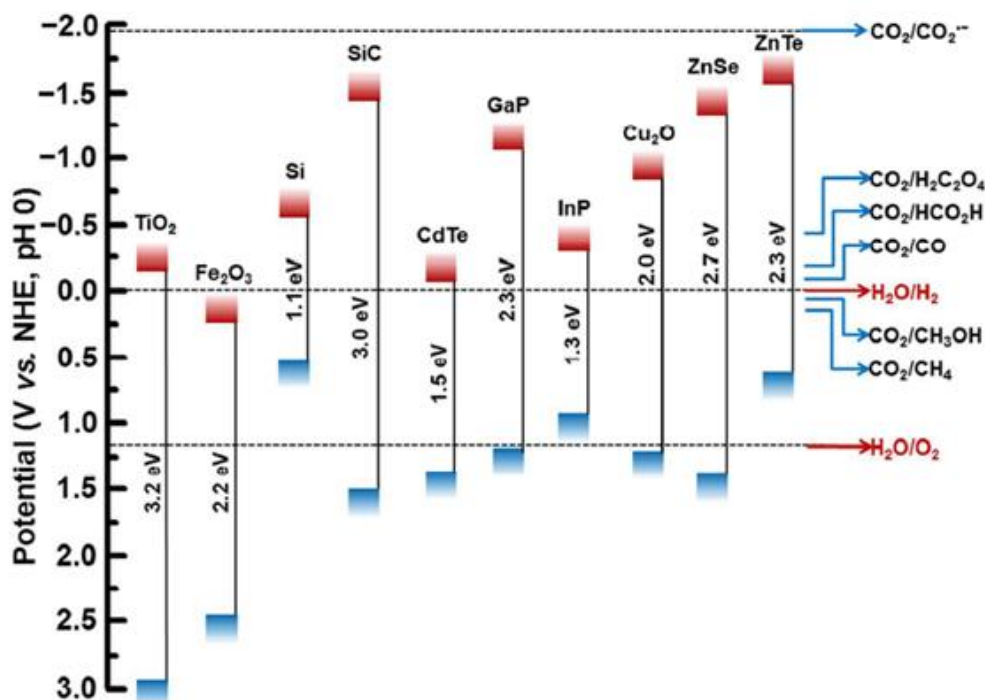


Figure 10. Conduction band (in red) and valence band (in blue) positions of some semiconductors and the redox potentials (vs. NHE) for CO₂ reduction and water splitting at pH= 0.⁶⁴

Barton et al.⁹⁰ presented a selective and efficient conversion of CO₂ to CH₃OH at a *p*-type semiconductor electrode made of a narrow band single crystal *p*-GaP (111) in a pyridine solution. The current efficiency is 100% at -0.3 V vs. SCE. Recently, Yu et al.⁹¹ developed a novel material by depositing a conformal, ultrathin, amorphous TiO₂ film by low-temperature atomic layer deposition on top of black Si. A photocurrent density of 32.3 mA·cm⁻² at an external potential of 0.87 V vs. SCE (1.48 V vs. RHE) in 1 M NaOH electrolyte could be achieved. ZnO, a *n*-type semiconductor with a wide band gap energy has been also tested as photocatalytic material due to its photo-luminescence properties (including good transparency and high electron mobility) that shows potential for scintillator applications.¹⁶ WO₃ is also suitable and stable enough for sustained reduction of CO₂. A PEC system using WO₃ as photoanode and Cu or Sn/SnO_x as a cathode has been shown to achieve reduction of CO₂ at low bias potentials under visible light.⁹² Si is

1
2
3 under visible-light in the presence of water, using a Ru(II)-Re(I) photo-cathode and a
4
5 CoO_x/TaON photoanode.
6
7

10 **Main reduction products**

11
12 The most common products from the photoelectrochemical reduction of CO₂ are
13 summarized hereafter. H₂ is a side reaction in CO₂ electroreduction, and so it is not
14
15 thoroughly discussed in the section.
16
17
18
19
20
21

22 *Carbon monoxide*

23
24 CO₂ reduction to CO can be seen as the simplest route for CO₂ conversion. CO is also an
25 intermediate product for the synthesis of other products, such as CH₃OH and hydrocarbon
26
27 fuels.⁹⁶ Petit and co-workers⁹⁷ proposed the reduction CO₂ to CO in a photocathode-dark
28
29 anode configuration using two systems: *p*-GaAs/0.1 M KClO₄, H₂O, Ni(cyclam)²⁺ and *p*-
30
31 GaP/0.1 M NaClO₄, H₂O, Ni(cyclam)²⁺, which assist a selective photo-reduction at -0.44
32
33 V vs. SCE (-0.2V vs. SHE) using an anode of Pt, separated from the working-electrode
34
35 compartment by glass frits. Using a similar photocathode (*p*-GaAs)-dark anode (Pt) cell
36
37 configuration as Petit and co-workers in a one compartment cell, Hirota et al.⁹⁸ reduced
38
39 CO₂ to CO photoelectrochemically in CO₂ + CH₃OH at high-pressure conditions (40
40
41 atm). *P*-InP and *p*-Si as photoelectrodes were tested at different applied potentials. For 50
42
43 mA·cm⁻², *p*-InP required -1.1 V, *p*-GaAs -1.6 V and *p*-Si -1.8 V, demonstrating that CO₂
44
45 can be converted to CO at more positive potentials than for a Cu under similar
46
47 experimental conditions and without illumination. Moreover, Kumar and co-workers⁹⁹
48
49 using a one compartment cell configuration and a *p*-type H-Si photocathode with a
50
51 Re(bipy-But)(CO)₃Cl (bipy-But) 4,4'-di-tert-butyl-2,2'-bipyridine electrocatalyst
52
53 achieved a 600 mV lower potential (FE= 97%) than with a Pt electrode. The photocathode
54
55
56
57
58
59
60

1
2
3 + anode electrode configuration is usually employed to produce CO, since two-electron
4
5 chemical products are commonly found over p-type semiconductors. More recently,
6
7 Sahara et al.⁹⁵ generated CO using a dual photocathode-photoanode cell configuration
8
9 with an external electrical (0.3 V) and chemical bias (0.10 V) in a hybrid photocathode
10
11 of NiO-RuRe and a photoanode of CoO_x/TaON. The work can be considered the first
12
13 example of a molecular-semiconductor hybrid PEC cell using water to reduce CO₂.
14
15 Different photoelectrodes, apart from those mentioned above, are also reported with good
16
17 results such as p-type silicon nanowire with nitrogen-doped graphene quantum sheets (N-
18
19 GQSS);¹⁰⁰ p-GaAs and p-InP;¹⁰¹ CoSn(OH)₆;¹⁰² and NiO-RuRe.¹⁰³ Figure 11 compares
20
21 the FEs reported in literature for CO for the different electrode configurations in the PEC:
22
23 photocathode-dark anode (PC+A), photoanode-dark cathode (PA+C) and photocathode-
24
25 photoanode (PA+PC). The results seem to show an enhanced reaction performance for a
26
27 PC+A configuration.
28
29
30
31
32
33
34
35
36
37

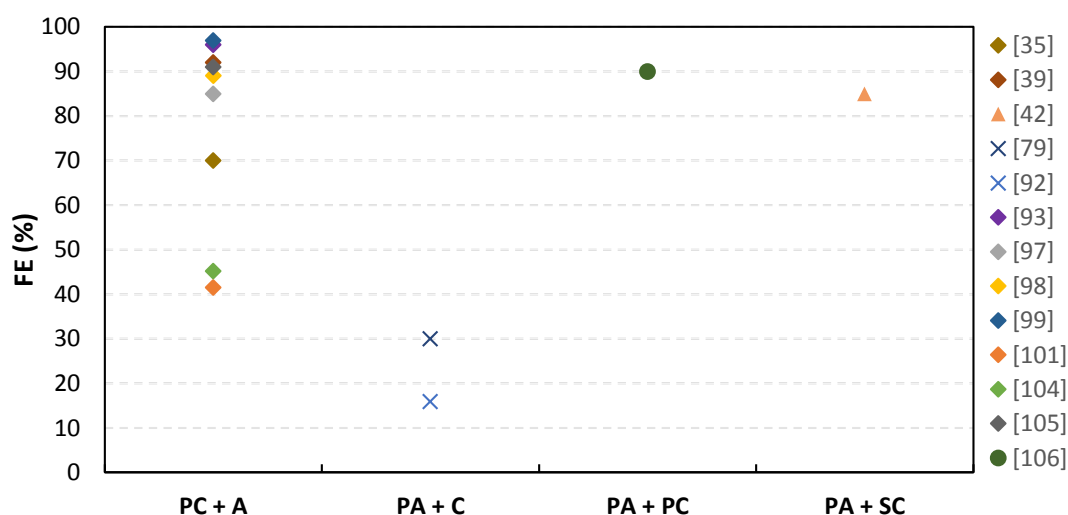


Figure 11. FEs for CO at different electrode configurations in PEC cells.

Formic Acid

Particular reference is made in the literature to the formation of HCOOH, this being a product for which there is a growing demand and which is currently made by processes that are neither straightforward nor environmentally friendly.¹² Morikawa and co-workers⁹⁴ successfully achieved the photoreduction of CO₂ to HCOOH without applying any electrical bias, employing a photocathode-photoanode configuration separated by a PEM membrane, using water as a proton source and electron donor by conjugating a InP/Ru-complex for CO₂ reduction with a TiO₂ photocatalyst for water oxidation. HCOOH was generated continuously with a FE of > 75%. However, the TiO₂ high band gap critically reduce its excitation wavelength to the UV range. Jiang et al.¹⁰⁷ expanded the TiO₂ optical absorption region from the UV absorption to the visible light region by depositing Fe₂O₃ (Fe₂O₃/TiO₂ NTs) with an onset wavelength of ~600 nm. The maximum selectivity was 99.89% with a rate of HCOOH production of 74896.13 nmol·h⁻¹·cm⁻² under optimal conditions in a photocathode-dark anode dual chamber cell using Pt as counter electrode. Employing a similar photoelectroreactor configuration, Gu and co-workers¹⁰⁸ reduced CO₂ to HCOOH without the need for a co-catalyst at an unparalleled underpotential. However, FE was limited due to the competitive reaction for H₂ formation (HER). In his work, a *p*-type Mg-doped CuFeO₂ electrode was found to reduce CO₂ to HCOOH photoelectrochemically with a maximum conversion efficiency at -0.9 V vs. SCE using a LED source (470nm) in experiments of 8 to 24 hours. Shen and co-workers¹⁰⁹ reported in 2015 one of the highest yields to HCOOH. In this work, CO₂ was reduced using a photocathode-dark anode configuration at Cu nanoparticles decorated with Co₃O₄ nanotube arrays achieving a selectivity of nearly 100% employing a single compartment cell. The production of HCOOH was as high as 6.75 mmol·L⁻¹·cm⁻² in 8 h of experimental time. One year later, Huang et al.⁶⁶ improved the yield reported by Qi Shen and co-

workers employing also Co_3O_4 as the light harvester, and $\text{Ru}(\text{bpy})_2\text{dppz}$ as the electron transfer mediator and CO_2 activator. The photoelectroreduction of CO_2 to HCOOH has been realized for 8 hours with an onset potential as low as -0.69 V vs. SCE (-0.45 V vs. NHE) and an anode made of graphite. At an applied potential of -0.84 V vs. SCE (-0.60 V vs. NHE), the selectivity for HCOOH reached 99.95%, with a FE of 86% and a production of $110 \mu\text{mol}\cdot\text{cm}^{-2}\cdot\text{h}^{-1}$.

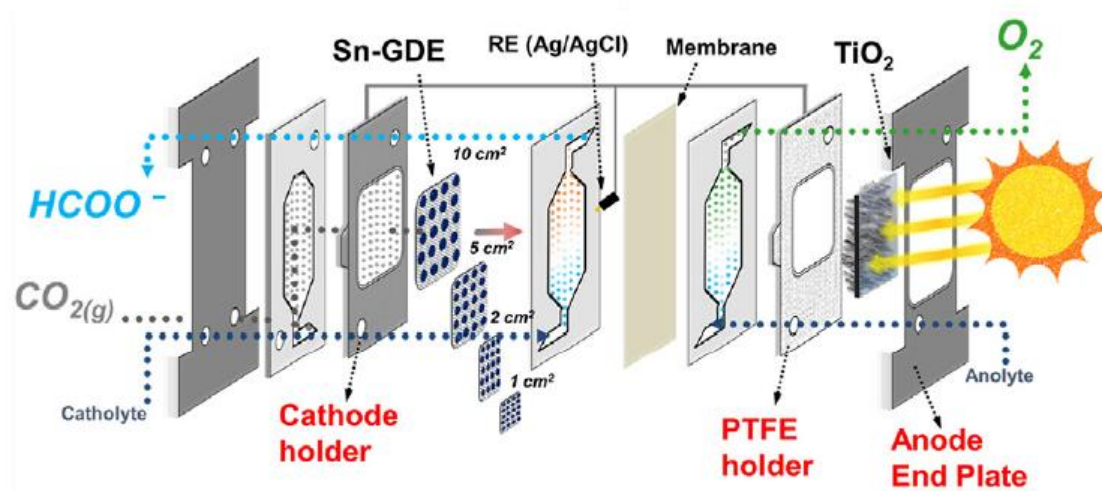


Figure 12. Photoelectrochemical flow cell scheme using a TiO_2 photoanode.¹¹⁰

Nowadays, improvements in HCOOH formation continues with new strategies. Irtem and co-workers, continuing with their research line using Sn,^{110, 111} proposed two strategies: concentration of solar light on the photoanode and adjustment of cathode area. At a voltage of 1.2 V and with a TiO_2 photoanode and a Sn cathode, FEs of 40-65% for HCOO^- production were obtained, with energy efficiencies as high as 70% using a two-compartment cell divided (Figure 12). This study demonstrated that a stable photoanode optimized the system efficiency using a GDE as a cathode to enhance mass transfer and provide a wide photovoltage for O_2 evolution reaction (OER). Besides, three PEC cell

electrode configurations can be found in literature for HCOOH production, where PC+A seems to be beneficial as it is observed for HCOOH production (Figure 13).

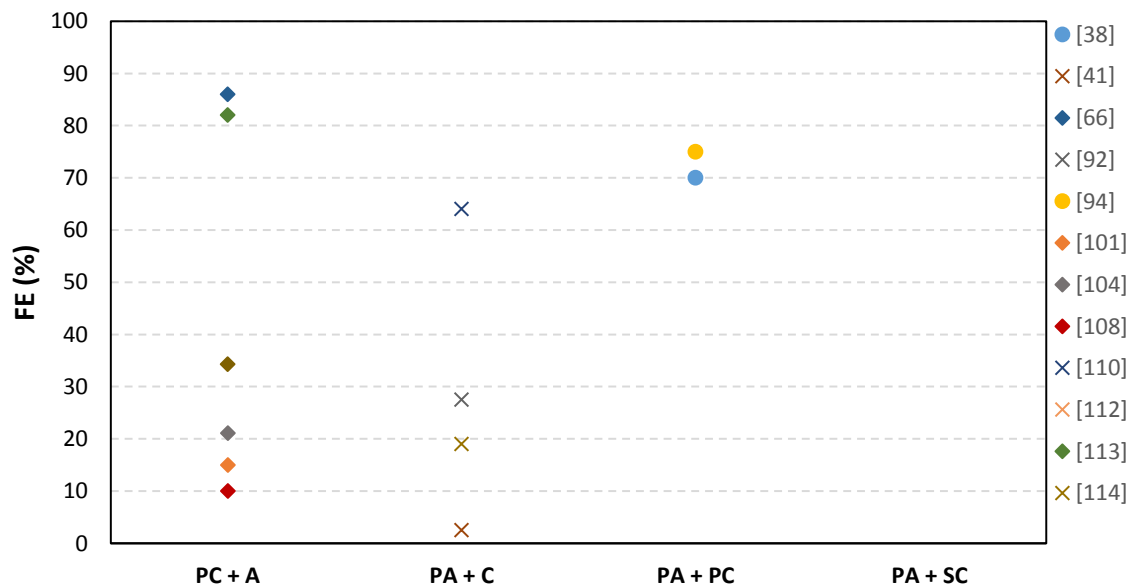


Figure 13. FEs for HCOOH at different electrode configurations in PEC cells.

Methanol

CH₃OH as a key commodity has become an important part of our global economy. Several articles deal with CH₃OH production¹¹⁵⁻¹¹⁷ since it may directly replace fossil fuels without modifications of the actual energy distribution infrastructure.^{3, 96, 118} Moreover, CH₃OH is used in paints, building blocks for plastics, and organic solvents, among others. Ogura and Uchida¹⁴ were one of the first reporting the formation of CH₃OH by photoelectroreduction of CO₂ using a *n*-TiO₂ photoanode and a metal complex-confined Pt cathode separated by a PEM and a 500 W Xe lamp. In their experiments, it was observed that the feasibility for CO₂ reduction in a photocell depended mainly on the anolyte pH. pH higher than 12 led to CH₃OH formation in the

1
2
3 cathode , and O₂ evolved at the photoanode. The photoreduction of CO₂ only occurred at
4
5 a pH below 11 when applying external energy.
6
7

8
9
10 Yuan et al.¹¹⁹ proposed the photoelectroreduction of CO₂ using a Cu₂O photocathode and
11
12 a graphite sheet as dark anode, obtaining a concentration and FE for CH₃OH formation
13
14 of 1.41 mmol and 29.1%, respectively, after 1.5 h of operation at 1.5 V vs. SCE in a single
15
16 compartment cell with an irradiation of 100 mW·cm⁻² emitted from a Xe lamp. The
17
18 formation rate of CH₃OH was 23.5 μmol·cm⁻²·h⁻¹. A higher rate for CH₃OH (45 μmol·cm⁻²·h⁻¹)
19
20 was achieved in a light-driven two compartment reactor using Cu₂O/graphene/TiO₂
21
22 nanotube array (TNA) heterostructures and Pt as working electrode and counter electrode,
23
24 respectively by Li et al.⁴⁰ An intensity of 100 mW·cm⁻² was applied by a 300 W Xe arc
25
26 lamp with a UV cutoff filter. Similar materials, but with different structure and in a single
27
28 compartment cell, were employed by Lee and co-workers,¹²⁰ enhancing FE and stability
29
30 towards CH₃OH production from CO₂ using Cu₂O nanowires photocathodes with a TiO₂-
31
32 Cu⁺ shell. The FE after 2 h of operation improved from 23.6% for a Cu₂O photocathode
33
34 to 56.5% for Cu₂O with a TiO₂-Cu⁺ shell mainly due to a lower resistance to charge
35
36 transfer and an increased CO₂ adsorption. Recently, Yang et al.¹²¹ compared the CH₃OH
37
38 formation at different catalytic processes (PEC, photocatalysis, electrocatalysis) on a
39
40 SnO₂ NRs/Fe₂O₃ NTs photocathode and a Pt wire anode employing a single compartment
41
42 cell. The largest CH₃OH production (2.05 mmol·L⁻¹·cm⁻²), obtained under visible light
43
44 (1.1 V extra) was far higher than that individually electro-or-photo-catalytic reduction.
45
46 As it is the case for CO and HCOOH, the production of CH₃OH can be enhanced with a
47
48 PC+A configuration (Figure 14). The extraordinary high FE obtained for CH₃OH
49
50 formation (i.e. >100%) for PA+C system using TiO₂ as photoanode and Pt as cathode,¹⁴
51
52
53
54
55
56
57
58
59
60 has been removed for a clear comparison.

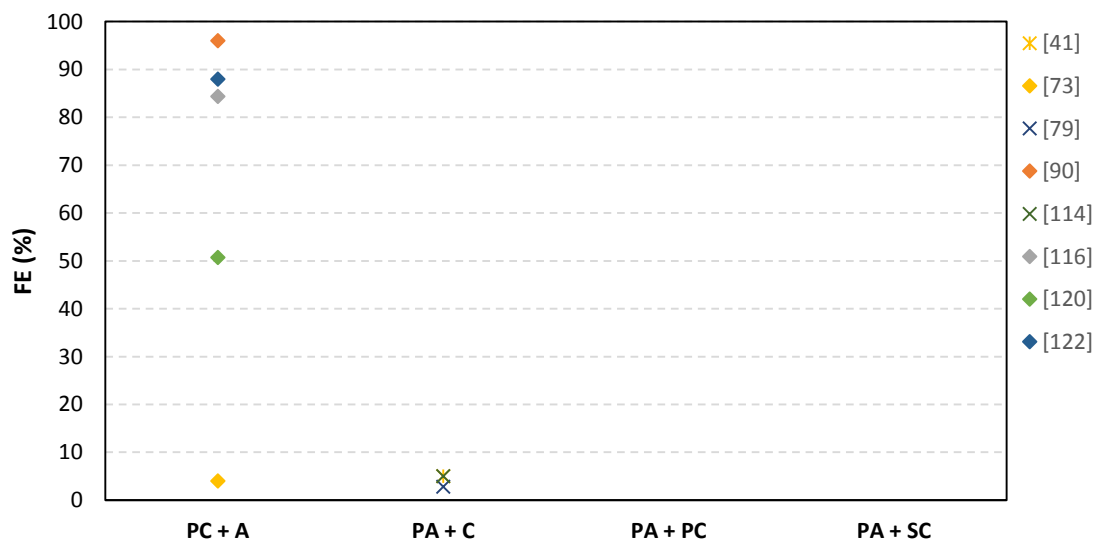


Figure 14. FEs for CH₃OH at different electrode configurations in PEC cells.

Methane

Kaneco et al.¹⁰⁴ demonstrated that the selectivity for the photoelectrochemical reduction of CO₂ can be tuned by adding metal particles into the catholyte to form CH₄ in a dual compartment cell by adding Cu particles suspended CH₃OH using a *p*-InP and a Pt foil as photocathode and anode, respectively. A maximum FE for CH₄ of 0.56% was achieved at 265K under a 5000 W Xe lamp. In order to enhance the CH₄ production efficiency, Wang and co-workers⁸⁸ presented the use of ordered mesoporous TiO₂ as photocathode and Pt as anode for CO₂ reduction to CH₄. The ordered mesoporous TiO₂ exhibits a higher and stable production efficiency for CH₄ (0.192 μmol·g_{catalyst}⁻¹·h⁻¹) which is 71 and 53 times higher than that for a commercial TiO₂ (P25) and disordered mesoporous TiO₂, respectively. Employing a photoanode-dark cathode electrode configuration in a dual cell compartment, a FE of 67% for CH₄ at -1.39 V vs. SCE (-0.75 V vs. RHE) and 71.6% for all carbon-containing products at -1.34 V vs. SCE (-0.65 V vs. RHE) was achieved by

1
2
3 Magesh et al.⁹² using Cu as a cathode electrocatalyst and WO₃ as photoanode under bias
4 potential. Moreover, in a photocathode-dark anode electrode configuration, Ong and co-
5 workers⁴⁴ reached 2.923 $\mu\text{mol}\cdot\text{g}_{\text{catalyst}}^{-1}\cdot\text{h}^{-1}$ of CH₄ under visible light irradiation
6 employing a carbon nanodot/g-C₃N₄ (CND/pCN) hybrid heterojunction photocatalyst
7 with a mass loadings of 3% of CNDs and a Pt foil as anode. This improved in 3.6 times
8 the CH₄ generated with pCN pure. Thompson et al,¹²³ reported an initial conversion rate
9 of 2596 $\mu\text{L}\cdot\text{g}_{\text{catalyst}}^{-1}\cdot\text{h}^{-1}$ of CH₄, the highest reported to date, employing Cu as cathode
10 and TiO₂ as photoanode without using an external wire. Only UV light as an energy
11 source was employed to reduce CO₂. In any case, FEs to CH₄ are rarely reported with
12 values ranging from 54.6 to 67 % for a PA+C configuration.^{79, 92}

28 *Long chain hydrocarbons.*

30 Attending to thermodynamics, CO₂ reduction to long chain hydrocarbons is more
31 challenging because of the number of electron required.⁴ For instance, CO₂ reduction to
32 CH₃OH requires 6-electron process, while CO₂ reduction to isopropanol is a 18-electron
33 reduction. These liquid fuels have higher energy densities and are more convenient for
34 transport and storing. Ampelli et al.^{37, 124} reduced CO₂ to liquid fuels (mainly
35 CH₃CH(OH)CH₃) employing carbon-nanotube based electrodes, Pt/CNT and Fe/CNT
36 and nanostructured TiO₂ as photoanode in a homemade Plexiglas-quartz window PEC
37 reactor, reaching a production of $2.28\cdot 10^{-2}\cdot\mu\text{mol}\cdot\text{h}^{-1}\cdot\text{cm}^{-2}$ of CH₃CH(OH)CH₃ for the
38 Fe/CNT cathode. As it can see in Figure 15, better results were achieved when instead of
39 Fe-CNT, Fe-nitrogen-doped carbon nanotubes were employed ($5.74\cdot 10^{-2}\mu\text{mol}\cdot\text{h}^{-1}\cdot\text{cm}^{-2}$).

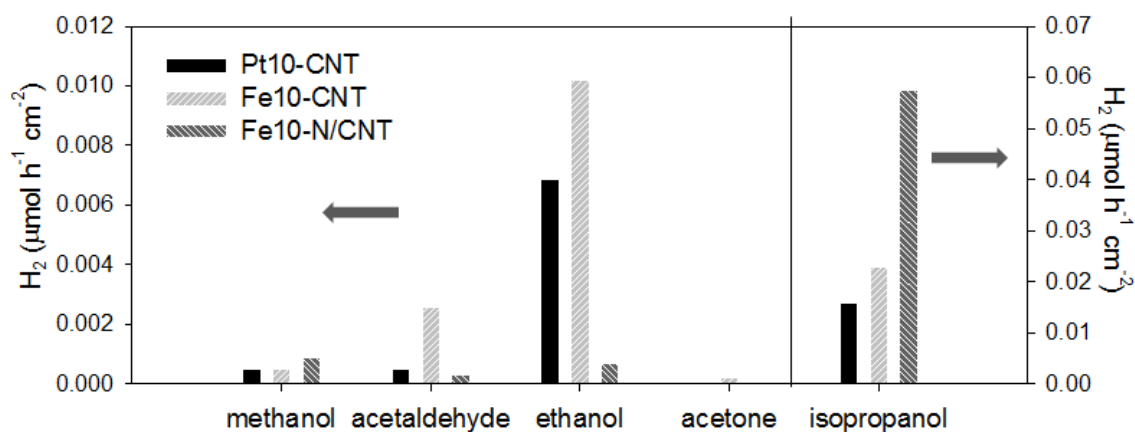


Figure 15. Electroreduction of CO₂ in the gas phase over Nafion® 117/Pt or Fe(10%)/CNT)20%/carbon GDEs.¹²⁴

Genovese et al.⁵⁷ employed the same material but operated under a gas-phase electrocatalytic cell using electrodes based on metal nanoparticles supported and TiO₂ as photo-anode. Long C-chain products (i.e. CH₃CH(OH)CH₃ and C₈-C₉) were obtained from CO₂. Employing also a TiO₂ photoanode and a nanostructured Pt/graphene aerogel deposited onto a Cu foam (Pt/GA/CF), Zhang and co-workers¹¹⁴ revealed that the Pt/GA/CF electrode improved CO₂ reduction significantly and facilitated the conversion of C₁ to high-order products due to enhanced charge transportation. HCOOH, CH₃COOH, C₂H₅COOH, CH₃OH, C₂H₅OH were the main products detected. Recently, Yuan et al.¹²⁵ showed in his study an outstanding performance for C₂H₅OH production. At the Cu₂O foam cathode, the solar driven conversion of CO₂ to C₂H₅OH led to a formation rate as high as 71.67 μmol·cm⁻²·h⁻¹ at only 131 mV within 1.5 h. There are a variety of FEs reported for different hydrocarbons, with values ranging from 32.6 to 52% for PC+A configurations^{59, 73} and 2.7 for 45% to PA+C configurations.^{41, 92, 114}

1
2
3 Finally, Tables 3, 4, 5 and 6 summarize the literature on the topic, paying special attention
4
5 to the photoelectron-reactor/electrode configuration, but also including
6
7 photoelectrocatalytic materials, main products obtained and process conditions.
8
9
10
11
12
13
14
15
16
17
18
19
20
21
22
23
24
25
26
27
28
29
30
31
32
33
34
35
36
37
38
39
40
41
42
43
44
45
46
47
48
49
50
51
52
53
54
55
56
57
58
59
60

Table 3. Experimental conditions and main products in a Photocathode-dark anode configuration.

Photocathode	Anode	Light source/ Intensity	Electrode Potencial (V vs. SCE)	Product	FE/ Productivity	Ref.
<i>p</i> -GaP	Carbon road	Hg-lamp ($\lambda=365$ nm)	-1 V	CH ₂ O HCOOH CH ₃ OH	-	15
<i>p</i> -GaAs	Pt	150W Tungsten lamp ($\lambda > 380$ nm)	-1.2 V	CO	47%	97
<i>p</i> -Gap	Pt		-1 V	CO	85%	
<i>p</i> -InP	Pt	500 W Xe lamp ($\lambda > 370$ nm)	-1.1 V	CO	89%.	98
<i>p</i> -GaAs	Pt		-1.6 V	CO	74%.	
<i>p</i> -Si	Pt		-1.8 V	CO	75%.	
<i>p</i> -InP/deposited-metal [Pb, Ag, Au, Pd, Cu and Ni]	Pt	5000 W Xe lamp ($\lambda > 300$ nm)	-2.5 V	CO HCOOH	-	77
<i>p</i> -GaAs	Pt	5000 W Xe lamp ($\lambda > 300$ nm)	-2.4 V	CO HCOO ⁻	CO: 24.9% HCOO ⁻ : 14%	101
<i>p</i> -InP			-2.5 V	CO HCOO ⁻	CO: 41.5% HCOO ⁻ : 15%	

<i>p</i> -GaP	Pyridine	200 W Hg-Xe arc light ($\lambda > 365$ nm)	-0.4 V	CH ₃ OH	88%-100%	90
<i>p</i> -InP	Pt	5000 W Xe lamp ($\lambda > 300$ nm)	-2.4 V to -2.8 V	CO HCOOH	CO at -2.7 V: 45.2% HCOOH at -2.6 V: 21.1%	104
<i>p</i> -Si	Pt	150 quartz halogen lamp ($\lambda < 1000$ nm)	-0.6 V	CO	97%	99
<i>p</i> -InP-Zn	[Ru(L- L)(CO) ₂] _n	Xe light (400 nm < $\lambda < 800$ nm)	-0.6 V	HCOO ⁻	34.3 %	112
Cu ₂ ZnSnS ₄ (CZTS)	[RuCE + RuCA	(400 nm < $\lambda < 800$ nm)	-0.4 V	HCOO ⁻	82 %	113
meso- tetraphenylporphyrin FeIII chloride at <i>p</i> -type Si	CF ₃ CH ₂ OH	Halogen fibre optic lamp ($\lambda_{\max} =$ 650 nm)	-1.1 V	CO	92%	39
Mg-doped CuFeO ₂	Pt	75 W Xe (350 nm < $\lambda > 1350$ nm)	-0.9 V	HCOO ⁻	10%	108

Cu/Cu ₂ O	Pt	125 W Hg lamp	0.2 V	CH ₃ OH	-	115
Cu/Cu ₂ O	Pt	LED light (435 nm λ 450 nm)	-2.0 V	CH ₄ C ₂ H ₄	C ₂ H ₄ : 32.69%	59
Wedged N-doped CuO	Pt	Xe lamp ($\lambda \geq 420$ nm)	-1.2 V	CH ₃ OH	84.4%	116
Ordered mesoporous TiO ₂	Pt	300 W Xe arc lamp	-0.4 V	CH ₄ CO	-	88
<i>p</i> -type CuO/Cu ₂ O	Stainless steel 378	(AM 1.5) Solar simulator (Newport Model 91160).	-0.3 V	C ₂ H ₅ OH C ₃ H ₈ O CH ₃ OH	C ₂ H ₅ OH:52% C ₃ H ₈ O:40% CH ₃ OH:4%	59
Cu/Cu ₂ O	Pt	125 W Hg lamp	0.20 V	CH ₃ OH C ₂ H ₅ OH CH ₂ O C ₂ H ₄ O CH ₃ COCH ₃	-	117
Cu-CO ₃ O ₄ NTs	Pt	300 W Xe lamp	-0.9 V	HCOO ⁻	-	109
Cu ₂ O-TiO _{2-x}	-	150 W Xe lamp (AM 1.5)	-0.07 V to -0.77 V	CH ₃ OH HCOOH	-	34
NiO	Pt	LED with an output of 1000 lm.	-0.4 V	H ₂	-	75

Ru(bpy) ₂ dppz-Co ₃ O ₄ /CA	graphite plate	Xe lamp ($\lambda > 420$ nm)	-0.84 V	HCOO ⁻	86%	66
1T@2H-MoS ₂	Pt	Visible-light illumination (400nm $\langle \lambda \rangle$ 800 nm)	-0.6 V	-	-	126
Au ₃ Cu NP/Si NW	-	-	-0.8 V	CO	-	127
Si Photoelectrode with the RA-Treated Au Thin Film Mesh	-	100 mW cm ⁻²	-0.73 V	CO	91%	105
Cu ₂ O/graphene/TNA	Pt	300 W Xe Arc lamp ($\lambda > 400$ nm)	-0.8 V vs. SCE	CH ₃ OH	45 $\mu\text{mol cm}^{-2} \text{h}^{-1}$	40
Ti/ZnO-Fe ₂ O ₃	Pt	300 W Xe lamp (400 nm $\langle \lambda \rangle$ 800 nm)	-0.5 V	CH ₃ OH HCOOH CH ₂ O	CH ₃ OH: 0.773 mmol/cm ²	74
Cu-ZnO/GaN/n ⁺ -p Si	-	300 W Xe lamp	-0.6 V	CO	70%	35
Cu ₂ O	Pt	LS 150 with AM1.5 G filter	-0.3 V	CH ₃ OH	23.6%	120
Cu ₂ O/TiO ₂ -Cu ⁺					50.7%	
CdSeTe NPs/TiO ₂ NTs	Pt	500W Xe lamp ($\lambda \geq 420$ nm)	-1.2 V	CH ₃ OH	88%	122
CdSeTe NSs/TiO ₂				CH ₃ OH	25%	

SnO ₂ NRs/Fe ₂ O ₃ NTs	Pt	Xenon lamp ($\lambda \geq 420$ nm)	-1.1 V	CH ₃ OH	87.04%	121
Cu ₂ O	Graphite sheet	100 mW cm ⁻²	-0.6 V	C ₂ H ₅ OH	0.071 mmol·cm ⁻² ·h ⁻¹	125
0D/2D CND/pCN	Pt	300 W Xe arc lamp ($\lambda > 400$ nm)	-0.5 V	CH ₄ CO	CH ₄ : 2.9 $\mu\text{mol} \cdot \text{g}_{\text{catalyst}}^{-1} \cdot \text{h}^{-1}$ CO: 5.8 $\mu\text{mol} \cdot \text{g}_{\text{catalyst}}^{-1} \cdot \text{h}^{-1}$	44
Si/Au	Graphite-rod	100 mW cm ⁻²	0 V	CO	96%	93

Table 4. Experimental conditions and main products in a Photoanode-dark cathode configuration.

Cathode	Photoanode	Light source/ Intensity	Electrode Potential (V vs. SCE)	Product	FE/ Productivity	Ref.
Pt	<i>n</i> -TiO ₂	500 W Xe- lamp	-2 V	CH ₃ OH	100%	14
Pt-RGO	Pt-TNT	300 W Xe-arc lamp	-2 V	C ₂ H ₅ OH CH ₃ COOH CH ₃ OH	CH ₃ OH: 5% HCOOH: 2.5% CH ₃ COOH: 20%	41

				HCOOH	C ₂ H ₅ OH:45%	
Cu	WO ₃	500 W Hg lamp ($\lambda > 420$ nm)	-1.39 V	CO CH ₄ C ₂ H ₄	CO: 0.6% CH ₄ :67% C ₂ H ₄ :2.7%	92
Sn/SnO _x			-1.34 V	CO HCOOH	CO:15.9% HCOOH:27.5%	
Pt-RGO/Cu	TiO ₂ nanotube	300 W Xe-arc lamp (320 nm< λ >410 nm)	-2 V	HCOOH CH ₃ COOH C ₂ H ₅ COOH CH ₃ OH C ₂ H ₅ OH	-	78
Pt-RGO	Pt-TNT	300 W Xe arc lamp (320 nm< λ >410 nm)	-2 V	C ₂ H ₅ OH CH ₃ COOH CH ₃ OH HCOOH CO	C ₂ H ₅ OH: 1350 nmol·cm ⁻² ·h ⁻¹ CH ₃ COOH: 1150 nmol·cm ⁻² ·h ⁻¹ CH ₃ OH: 875 nmol·cm ⁻² ·h ⁻¹ HCOOH: 820 nmol·cm ⁻² ·h ⁻¹ CO: 650 nmol·cm ⁻² ·h ⁻¹	128

Pt	Cu-RGO-TiO ₂ /ITO	150 W Xe arc lamp	-0.61 V	HCOOH CH ₃ OH	CH ₃ OH: 255 mmol·cm ⁻² ·h ⁻¹ HCOOH: 189.06 mmol·cm ⁻² ·h ⁻¹	129
Pt-RGO	Pt (5%)-TNT	300 W Xe arc lamp (320 nm< λ >410 nm)	-2 V	HCOOH CH ₃ OH CH ₃ COOH C ₂ H ₅ OH	HCOOH: 80 nmol·cm ⁻² ·h ⁻¹ CH ₃ OH: 75 nmol·cm ⁻² ·h ⁻¹ CH ₃ COOH: 250 nmol·cm ⁻² ·h ⁻¹ C ₂ H ₅ OH: 280 nmol·cm ⁻² ·h ⁻¹	65
Cu ₂ O	TiO ₂	100 mW·cm ⁻² AM 1.5G	-1.49 V	CH ₄ CO CH ₃ OH	CH ₄ : 54.63% CO:30.03% CH ₃ OH:2.79%	79
Pt	b-Si/TiO ₂ /Co(OH) ₂	150W Xe lamp light	1.04 V	-	-	91
Pt/GA/CF	TiO ₂	300 W Xe arc lamp (320 nm< λ >410 nm)	-2 V	HCOOH C ₃ COOH C ₂ H ₅ COOH	HCOOH: 19% CH ₃ COOH: 24% C ₂ H ₅ COOH:23%	114

				CH ₃ OH C ₂ H ₅ OH	CH ₃ OH: 5% C ₂ H ₅ OH: 29%	
Sn-GDE	TiO ₂	300 W Xe lamp	-1.2 V	HCOO ⁻	40–65%	110
Cu	TiO ₂ NWs	250 W lamp (λ<400 nm)	0 V	CH ₄	2596 μL·g _{catalyst} ⁻¹ ·h ⁻¹	123
Pd/C	GaAs/InGaP/Ti O ₂ /Ni	100 mW·cm ⁻² AM 1.5G	0 V	HCOO ⁻	94%	69

0

Table 5. Experimental conditions and main products in a Photocathode-Photoanode configuration.

Photocathode	Photoanode	Light source/Intensity	Electrode Potential (V vs. SCE)	Product	FE/ Productivity	Ref.
InP/[MCE]s	TiO ₂ /Pt	1 sun (AM 1.5)	0 V	HCOO ⁻	70%	38
<i>p</i> -type Si nanowire	<i>n</i> -type TiO ₂ nanotube	Photocathode: 150W Xe lamp (AM 1.5) Photoanode: 25W Hg arc lamp	-1.5 V	CO CH ₄ C ₄ H ₈ C ₂ H ₄ C ₃ H ₈ C ₄ H ₁₀	CO: 824 nmol/cm ² ·h CH ₄ : 121.5 nmol/cm ² ·h C ₂ H ₄ : 80 nmol/cm ² ·h	80
InP/Ru-complex	TiO ₂	1 sun, Air Mass 1.5	0 V	HCOO ⁻	75%	94
Si NWs@CoP/CN	TiO ₂ NWs@CoP/CN	-	-0.81 V	CO CH ₄	CO: 90%	106
NiO-RuRe	CoO _x /TaON	300 W Xe lamp ($\lambda > 460$ nm)	-0.3 V	CO	-	95

Table 6. Experimental conditions and main products in a PEC-Solar cell tandem configuration.

Photo/cathode	Photo/anode	Light source/Intensity	Electrode Potential (V vs. SCE)	Product	FE/ Productivity	Ref.
ZnTe-Based	Co-Ci	100 mW cm ⁻²	0 V	CO	-	130
GaN	Pt	300 W Xenon lamp	-	CH ₄	19 %	131
Cu _x O	WO ₃	200 W Xenon lamp (AM 1.5)	0 V	CO HCOO ⁻	-	132
Cu-Zn	Si/Ni	150 W Xenon lamp AM 1.5	0 V	CO	85 %	42

CONCLUSIONS AND FUTURE PERSPECTIVES

The photoelectrocatalytic reduction of CO₂ is a promising technological alternative that combines the advantages of electrocatalysis and photocatalysis, reducing the applied voltage needed in CO₂ conversion to useful chemical. Undoubtedly, many issues remain to be solved before photoelectrocatalysis processes come to reality, although the technology presents potential for an enhanced CO₂ reduction efficiency under the sun.

The design of a photoelectrochemical reactor should be made based on a careful evaluation of different factors, such as light source, geometrical configuration, construction material, heat exchange, mixing and flow characteristics, etc. Two key parameters in the process are the phases involved and the mode of operation (i.e., batch, semi-batch or continuous). Photocatalysts can be generally tested in either fluidized or fixed bed reactors. Besides, the anode and cathode in the photoelectrochemical device should be preferably in the form of thin films separated by a proton-conducting membrane and deposited over porous substrates, which allows an efficient collection/transport of electrons as well as the diffusion of protons through the membrane. For CO₂ photoreduction, an efficient evolution of oxygen on the anode side is also needed, as well as an efficient diffusion of CO₂ on the cathode side.

Photocathode-dark anode configuration has been commonly reported for CO₂ reduction. This configuration employs a photocathode made of a *p*-type semiconductor because of their high conduction band energy suitable for CO₂ reduction, but its efficiency is limited. In the last years, the photoanode-dark cathode configuration is being used more frequently due to the benefits of using *n*-type semiconductors instead of *p*-type

1
2
3 semiconductors, which are earth abundant, cheap and stable for H₂O oxidation. Another
4
5 option for the arrangement of the photoelectrodes in the PEC cells is the combination of
6
7 a photocathode made of a *p*-type semiconductor for CO₂ reduction with a photoanode
8
9 made of a *n*-type semiconductor for H₂O oxidation. This configuration, in contrast to
10
11 the other two, allows realizing the reduction of CO₂ with H₂O without an external
12
13 electric bias.
14
15
16
17
18
19

20 **ACKNOWLEDGEMENTS**

21
22
23 The authors would like to acknowledge the financial support from the Spanish Ministry
24
25 of Economy and Competitiveness (MINECO) under the project CTQ2016- 76231-C2-1-
26
27 R and Ramón y Cajal programme (RYC-2015-17080).
28
29
30

31 **REFERENCES**

- 32
33
34 (1) Peng, Y.P.; Yeh, Y.T.; Wang, P.Y.; Huang, C.P. A solar cell driven electrochemical
35
36 process for the concurrent reduction of carbon dioxide and degradation of azo dye in
37
38 dilute KHCO₃ electrolyte. *Sep. Purif. Technol.* **2013**, 117, 3–11,
39
40 10.1016/j.seppur.2013.03.044.
41
42
43 (2) Zheng, Y.; Zhang, W.; Li, Y.; Chen, J.; Yua, B.; Wang, J.; Zhang, L.; Zhang, J. Energy
44
45 related CO₂ conversion and utilization: Advanced materials/ nanomaterials, reaction
46
47 mechanisms and technologies. *Nano Energy* **2017**, 40, 512-539,
48
49 10.1016/j.nanoen.2017.08.049.
50
51
52 (3) Albo, J.; Alvarez-Guerra, M.; Castaño, P.; Irabien, A. Towards the electrochemical
53
54 conversion of carbon dioxide into methanol. *Green Chem.* **2015**, 17, 2304–2324,
55
56 10.1039/c4gc02453b.
57
58
59
60

- 1
2
3 (4) Albo, J.; Irabien, A. Cu₂O-loaded gas diffusion electrodes for the continuous
4 electrochemical reduction of CO₂ to methanol. *J. Catal.* **2016**, 343, 232-239,
5 10.1016/j.jcat.2015.11.014.
6
7
8
9
10 (5) Albo, J.; Beobide, G.; Castaño, P.; Irabien, A. Methanol electrosynthesis from CO₂ at
11 Cu₂O/ZnO prompted by pyridine-based aqueous solutions. *J. CO₂ Util.* **2017**, 18, 164-
12 172, 10.1016/j.jcou.2017.02.003.
13
14
15
16 (6) Das, S.; Daud, W.M.A. Photocatalytic CO₂ transformation into fuel: A review on
17 advances in photocatalyst and photoreactor. *Renew. Sust. Energ. Rev.* **2014**, 39, 765-805,
18 10.1016/j.rser.2014.07.046.
19
20
21
22
23 (7) Harriman, A. Prospects for conversion of solar energy into chemical fuels: the concept
24 of a solar fuels industry. *Phil. Trans. R. Soc. A* **2013**, 371, 20110415-20110415,
25 10.1098/rsta.2011.0415.
26
27
28
29
30 (8) Yan, Y.; et al. Photoelectrocatalytic Reduction of Carbon Dioxide. In *Carbon Dioxide*
31 *Utilisation*; Styring, P., Quadrelli, E. A., Armstrong, K. Eds.; Elsevier B.V., 2015.
32
33
34
35 (9) Ibrahim, N.; Kamarudin, S.K.; Minggu, L.J. Biofuel from biomass via photo-
36 electrochemical reactions: An overview. *J. Power Sources* **2014**, 259, 33-42,
37 10.1016/j.jpowsour.2014.02.017.
38
39
40
41
42 (10) Graves, C.; Ebbesen, D.; Mogensen, M.; Lackner, S. Sustainable hydrocarbon fuels
43 by recycling CO₂ and H₂O with renewable or nuclear energy. *Renew. Sust. Energ. Rev.*
44 **2011**, 15, 1-23, 10.1016/j.rser.2010.07.014.
45
46
47
48 (11) Jiang, Z.; Xiao, Z.; Kuznetsov, V.L.; Edwards, P.P. Turning carbon dioxide into fuel.
49 *Phil. Trans. R. Soc. A* **2010**, 368, 3343-3364, 10.1098/rsta.2010.0119.
50
51
52
53 (12) Chaplin, R.P.S.; Wragg, A.A. Effects of process conditions and electrode material
54 on reaction pathways for carbon dioxide electroreduction with particular reference to
55
56
57
58
59
60

1
2
3 formate formation. *J. Appl. Electrochem.* **2003**, 33, 1107-1123,
4
5 10.1023/B:JACH.0000004018.57792.b8.

6
7
8 (13) Kumar, B.; Llorente, M.; Froehlich, J.; Dang, T.; Sathrum, A.; Kubiak, C.P.
9
10 Photochemical and Photoelectrochemical Reduction of CO₂. *Annu. Rev. Phys. Chem.*
11
12 **2012**, 63, 541-69, 10.1146/annurev-physchem-032511-143759.

13
14 (14) Ogura, K.; Uchida, H. Electrocatalytic reduction of CO₂ to methanol. *J. Electroanal.*
15
16 *Chem.* **1987**, 220, 333-337, 10.1016/j.jcat.2018.08.017.

17
18 (15) Halmann, M. Photoelectrochemical reduction of aqueous carbon dioxide on *p*-type
19
20 gallium phosphide in liquid junction solar cells. *Nature* **1978**, 275, 115-116,
21
22 10.1038/275115a0.

23
24 (16) Sudha, D.; Sivakumar, P. Review on the photocatalytic activity of various composite
25
26 catalysts. *Chem. Eng. Prog.: Process Intensification* **2015**, 97, 112-133,
27
28 10.1016/j.cep.2015.08.006.

29
30 (17) Nikokavoura, A.; Trapalis, C. Alternative photocatalysts to TiO₂ for the
31
32 photocatalytic reduction of CO₂. *Appl. Surf. Sci.* **2017**, 391, 149-174,
33
34 10.1016/j.apsusc.2016.06.172.

35
36 (18) Herron, J. A.; Kim, J.; Upadhye, A. A.; Huber, G. W.; Maravelias, C. T. A general
37
38 framework for the assessment of solar fuel technologies. *Energy Environ Sci.* **2015**, 8,
39
40 126-157, 10.1039/C4EE01958J.

41
42 (19) Herron, J. A.; Maravelias, C.T. Assessment of solar-to-fuels strategies:
43
44 photocatalysis and electrocatalytic reduction. *Energy Technol.* **2016**, 4, 1369-1391,
45
46 10.1002/ente.201600163.

47
48 (20) Yue, P.L. Introduction to the modelling and design of photoreactors. In
49
50 *Photoelectrochemistry, Photocatalysis and Photoreactors*; Schiavello, M., Eds.;
51
52 Springer: Dordrecht, 1985.

- 1
2
3 (21) Cassano, A.E.; Alfano, O.M. Design and Analysis of Homogeneous and
4 Heterogeneous Photoreactors. In: *Chemical Engineering: Trends and Developments*;
5 Galán, M. A.; Del Valle, E.M., Eds.; John Wiley & Sons, Ltd: Chichester, U.K., 2005.
6
7
8
9
10 (22) Bard, A.J. Photoelectrochemistry and heterogenous photo-catalysis at
11 semiconductors. *Journal of Photochem.* **1979**, 10, 59-75, 10.1016/0047-2670(79)80037-
12
13
14 4.
15
16
17 (23) Tryk, D.A.; Fujishima, A.; Honda, K. Recent topics in photoelectrochemistry:
18 achievements and future prospects. *Electrochim. Acta* **2000**, 45, 2363-2376,
19
20
21 10.1016/S0013-4686(00)00337-6.
22
23
24 (24) S. N. Habisreutinger; L. Schmidt-Mende; J. K. Stolarczyk. Photocatalytic Reduction
25 of CO₂ on TiO₂ and Other Semiconductors. *Angew. Chem. Int. Ed.* **2013**, 52, 2-39,
26
27
28 10.1002/anie.201207199.
29
30
31 (25) Zhao, J.; Wang, X.; Xu, Z.; Loo, J.S.C. Hybrid catalysts for photoelectrochemical
32 reduction of carbon dioxide: a prospective review on semiconductor/metal complex co-
33
34
35
36
37
38 (26) Highfield, J. Advances and Recent Trends in Heterogeneous Photo (Electro)-
39 Catalysis for Solar Fuels and Chemicals. *Molecules* **2015**, 20, 6739-6793,
40
41
42 10.3390/molecules20046739.
43
44
45 (27) Ampelli, C.; Centi, G.; Passalacqua, R.; Perathoner, S. Electrolyte-less design of
46 PEC cells for solar fuels: prospects and open issues in the development of cells and related
47
48
49
50
51
52 (28) Xie, S.; Zhang, Q.; Liu G.; Wang, Y. Photocatalytic and photoelectrocatalytic
53 reduction of CO₂ using heterogeneous catalysts with controlled nanostructures. *Chem.*
54
55
56
57
58
59
60
Commun. **2016**, 52, 35-59, 10.1039/C5CC07613G.

- 1
2
3 (29) Ozer, L.Y.; Garlisi, C.; Oladipo, H.; Pagliaro, M.; Sharief, S.A.; Yusuf, A.; Almheiri,
4 S.; Palmisano, G. Inorganic semiconductors-graphene composites in
5 photo(electro)catalysis: Synthetic strategies, interaction mechanisms and applications. *J.*
6 *Photochem. and photobiol. C: Photochem. Rev.* **2017**, *33*, 132-164,
7 10.1016/j.jphotochemrev.2017.06.003.
8
9
10 (30) Wang, P.; Wang, S.; Wang, H.; Wu, Z.; Wang, L. Recent Progress on Photo-
11 Electrochemical Reduction of Carbon Dioxide. Part. Part. Syst. Charact. **2018**, *35*,
12 1700371, 10.1002/ppsc.201700371.
13
14 (31) Chen, D.; Sivakumar, M.; Ray, A.K. Heterogeneous Photocatalysis in
15 Environmental Remediation. *Dev. Chem. Eng. Mineral Process.* **2000**, *8*(5/6), 505-550,
16 10.1002/apj.5500080507.
17
18 (32) Ampelli, C.; Passalacqua, R.; Perathoner, S.; Centi, G. Nano-engineered materials
19 for H₂ production by water photo-electrolysis. *Chem. Eng. Trans.* **2009**, *17*, 1011-1016,
20 10.3303/CET0917169.
21
22 (33) Ola, O.; Maroto-Valer, M.M. Review of material design and reactor engineering on
23 TiO₂ photocatalysis for CO₂ reduction. *J. Photochem. Photobiol C: Photochem. Rev.*
24 **2015**, *24*, 16-42, 10.1016/j.jphotochemrev.2015.06.001.
25
26 (34) Szaniawsk, E.; Bienkowskia, K.; Rutkowsk, I.A.; Kulesza, P.J.; Solarsk, R.
27 Enhanced photoelectrochemical CO₂-reduction system based on mixed Cu₂O-
28 nonstoichiometric TiO₂ photocathode. *Catal. Today* **2018**, *300*, 145-151,
29 10.1016/j.cattod.2017.05.099.
30
31 (35) Chu, S.; Fan, S.; Wang, Y.; Rossouw, D.; Wang, Y.; Botton, G.A.; Mi, Z. Tunable
32 Syngas Production from CO₂ and H₂O in an Aqueous Photoelectrochemical Cell. *Angew.*
33 *Chem. Int. Ed.* **2016**, *55*, 1-6, 10.1002/anie.201606424.
34
35
36
37
38
39
40
41
42
43
44
45
46
47
48
49
50
51
52
53
54
55
56
57
58
59
60

- 1
2
3 (36) Li, K.; Peng, B.; Peng, T. Recent Advances in Heterogeneous Photocatalytic CO₂
4 Conversion to Solar Fuels. *ACS Catal.* **2016**, *6*, 7485-7527, 10.1021/acscatal.6b02089.
5
6
7 (37) Ampelli, C.; Centi, G.; Passalacqua, R.; Perathoner, S. Synthesis of solar fuels by a
8 novel photoelectrocatalytic approach. *Energy Environ. Sci.* **2010**, *3*, 292-301,
9 10.1039/B925470F.
10
11
12 (38) Sato, S.; Arai, T.; Morikawa, T.; Uemura, K.; Suzuki, M.; Tanaka, H.; Kajino, T.
13 Selective CO₂ Conversion to Formate Conjugated with H₂O Oxidation Utilizing
14 Semiconductor/Complex Hybrid Photocatalysts. *J. Am. Chem. Soc.* **2011**, *133*, 15240-
15 15243, 10.1021/ja204881d.
16
17 (39) Alenezi, K.; Ibrahim, K.; Li, P.; Pickett, J. Solar Fuels: Photoelectrosynthesis of CO
18 from CO₂ at *p*-Type Si using Fe Porphyrin Electrocatalysts. *Chem. Rev.* **2010**, *110*, 6446-
19 6473, 10.1002/chem.201300764.
20
21 (40) Li, F.; Zhang, L.; Tong, J.; Liu, Y.; Xu, S.; Cao, Y.; Cao, S. Photocatalytic CO₂
22 conversion to methanol by Cu₂O/graphene/TNA heterostructure catalyst in a visible-
23 light-driven dual-chamber reactor. *Nano energy* **2016**, *27*, 320-329,
24 10.1016/j.nanoen.2016.06.056.
25
26 (41) Cheng, J.; Zhang, M.; Wu, G.; Wang, X.; Zhou, J.; Cen, K. Photoelectrocatalytic
27 Reduction of CO₂ into Chemicals Using Pt-Modified Reduced Graphene Oxide
28 Combined with Pt-Modified TiO₂ Nanotubes. *Environ. Sci. Technol.* **2014**, *48*, 7076-
29 7084, 10.1021/es500364g.
30
31 (42) Urbain, F.; Tang, P.; Carretero, N. M.; Andreu, T.; Gerling, L. G.; Voz, C.; Arbiol,
32 J.; Morante, J. R. A prototype reactor for highly selective solar-driven CO₂ reduction to
33 synthesis gas using nanosized earth-abundant catalysts and silicon photovoltaics. *Energy*
34 *Environ. Sci.* **2017**, *10*, 2256, 10.1039/C7EE01747B.
35
36
37
38
39
40
41
42
43
44
45
46
47
48
49
50
51
52
53
54
55
56
57
58
59
60

- 1
2
3 (43) Schreier, M.; Héroguel, F.; Steier, L.; Ahmad, S.; Luterbacher, J. S.; Mayer, M. T.;
4
5 Luo, J.; Grätzel, M. Solar conversion of CO₂ to CO using Earth-abundant electrocatalysts
6 prepared by atomic layer modification of CuO. *Nature Energy* **2017**, 2, 17087,
7
8 10.1038/nenergy.2017.87.
9
10
11 (44) Ong, W.J.; Putri, L.K.; Tan, Y.C.; Tan, L.L.; Li, N.; Ng, Y.H.; Wen, X.; Chai, S. P.
12 Unravelling charge carrier dynamics in protonated g-C₃N₄ interfaced with carbon
13 nanodots as co-catalysts toward enhanced photocatalytic CO₂ reduction: A combined
14 experimental and first-principles DFT study. *Nano Res.* **2017**, 10(5), 1673-1696,
15
16 10.1007/s12274-016-1391-4.
17
18 (45) Usubharatana, P.; McMartin, D.; Veawab, A.; Tontiwachwuthikul, P. Photocatalytic
19 Process for CO₂ Emission Reduction from Industrial Flue Gas Streams. *Ind. Eng. Chem.*
20
21 *Res.* **2006**, 45, 2558-2568, 10.1021/ie0505763.
22
23 (46) Nguyen, T.V.; Yu, J.C.S. Photoreduction of CO₂ in an optical-fiber photoreactor:
24 Effects of metals addition and catalyst carrier. *Appl. Catal., A* **2008**, 335, 112-120,
25
26 10.1016/j.apcata.2007.11.022.
27
28 (47) Du, P.; Carneiro, J.T.; Moulijn, J.A.; Mul, G. A novel photocatalytic monolith reactor
29 for multiphase heterogeneous photocatalysis. *Appl. Catal., A* **2008**, 334, 119-128,
30
31 10.1016/j.apcata.2007.09.045.
32
33 (48) Perego, C.; Peratello, S. Experimental methods in catalytic kinetics. *Catal. Today*
34
35 **1999**, 52, 133-145, 10.1016/S0920-5861(99)00071-1.
36
37 (49) Mukherjee, P. S.; Ray, A. K. Major Challenges in the Design of a Large-Scale
38 Photocatalytic Reactor for Water Treatment. *Chem. Eng. Technol.* **1999**, 22 (3), 253-260,
39
40 10.1002/(SICI)1521-4125(199903)22:3<253::AID-CEAT253>3.0.CO;2-X.
41
42
43
44
45
46
47
48
49
50
51
52
53
54
55
56
57
58
59
60

- 1
2
3 (50) Gerven, T.V.; Mul, G.; Moulijn, J.; Stankiewicz, A. A review of intensification of
4 photocatalytic processes. *Chem. Eng. Prog.* **2007**, 46, 781-789,
5 10.1016/j.cep.2007.05.012.
6
7
8
9
10 (51) Lin, H.; Valsaraj, K.T. An Optical Fiber Monolith Reactor for Photocatalytic
11 Wastewater Treatment. *AIChE J.* **2006**, 52 (6), 2271-2280, 10.1002/aic.10823.
12
13
14 (52) Sun, R.; Nakajima, A.; Watanabe, I.; Watanabe, T.; Hashimoto, K. TiO₂-coated
15 optical fiber bundles used as a photocatalytic filter for decomposition of gaseous organic
16 compounds. *J. Photochem. Photobiol. A: Chemistry* **2000**, 136, 111-116, 10.1016/S1010-
17 6030(00)00330-0.
18
19
20
21
22
23 (53) Kondratenko, E.V.; Mul, G.; Baltrusaitis, J.; Larrazábal, G. O.; Pérez-Ramírez, J.
24 Status and perspectives of CO₂ conversion into fuels and chemicals by catalytic,
25 photocatalytic and electrocatalytic processes. *Energy Environ. Sci.* 2013, 6:3,112-3135,
26 10.1039/C3EE41272E.
27
28
29
30
31
32
33 (54) Merino-Garcia, I.; Alvarez-Guerra, E.; Albo, J.; Irabien, A. Electrochemical
34 membrane reactors for the utilization of carbon dioxide. *Chem. Eng. J.* **2016**, 305, 104-
35 120, 10.1016/j.cej.2016.05.032.
36
37
38
39
40 (55) Delacourt, C.; Ridgway, P.L.; Kerr, J.B.; Newman, J. Design of an electrochemical
41 cell making syngas (CO + H₂) from CO₂ and H₂O reduction at room temperature. *J.*
42 *Electrochem. Soc.* **2008**, 155, B42-B49, 10.1149/1.2801871.
43
44
45
46 (56) Currao, A. Photoelectrochemical Water Splitting. *Chimia* **2007**, 61, 815-819,
47 10.2533/chimia.2007.815.
48
49
50
51 (57) Genovese, C.; Ampelli, C.; Perathoner, S.; Centi, G. Electrocatalytic conversion of
52 CO₂ to liquid fuels using nanocarbon-based electrodes. *J. Energ. Chem.* **2013**, 22, 202-
53 213, 10.1016/S2095-4956(13)60026-1.
54
55
56
57
58
59
60

- 1
2
3 (58) Singh, M. R.; Clark, E. L.; Alexis T. Bell, A. T. Effects of electrolyte, catalyst, and
4 membrane composition and operating conditions on the performance of solar-driven
5 electrochemical reduction of carbon dioxide. *Phys.Chem.Chem.Phys.* **2015**, 17, 18924-
6 18936, 10.1039/C5CP03283K.
7
8
9
10
11 (59) Ba, X.; Yan, L.; Huang, S.; Yu, J.; Xia, X.; Yu, Y. New Way for CO₂ Reduction
12 under Visible Light by a Combination of a Cu Electrode and Semiconductor Thin Film:
13 Cu₂O Conduction Type and Morphology Effect. *J. Phys. Chem. C* **2014**, 118, 24467-
14 24478, 10.1021/jp5063397.
15
16
17
18
19 (60) Kim, B.; Hillman, F.; Ariyoshi, M.; Fujikawa, S.; Kenis, P. J. A. Effects of
20 composition of the micro porous layer and the substrate on performance in the
21 electrochemical reduction of CO₂ to CO. *J. Power Sources* **2016**, 312, 192-198,
22 10.1016/j.jpowsour.2016.02.043.
23
24
25
26
27 (61) Del Castillo, A.; Alvarez-Guerra, M.; Irabien, A. Continuous Electroreduction of
28 CO₂ to Formate Using Sn Gas Diffusion Electrodes. *AIChE Journal* **2014**, 60, 3557-3564,
29 10.1002/aic.14544.
30
31
32
33 (62) Salvatore, D. A.; Weekes, D. M.; He, J.; Dettelbach, K. E.; Li, Y. C.; Mallouk, T.
34 E.; Berlinguette, C. P. Electrolysis of Gaseous CO₂ to CO in a Flow Cell with a Bipolar
35 Membrane. *ACS Energy Lett.* **2018**, 3, 149–154, 10.1021/acseenergylett.7b01017.
36
37
38
39 (63) Merino-Garcia, I.; Albo, J.; Irabien, A. Tailoring gas-phase CO₂ electroreduction
40 selectivity to hydrocarbons at Cu nanoparticles. *Nanotech.* **2018**, 29, 014001,
41 10.1088/1361-6528/aa994e.
42
43
44
45 (64) Chang, X.; Wang, T.; Gong, J. CO₂ Photo-reduction: Insights into CO₂ Activation
46 and Reaction on Surfaces of Photocatalysts. *Energy Environ. Sci.* **2016**, 9, 2177-2196,
47 10.1039/C6EE00383D.
48
49
50
51
52
53
54
55
56
57
58
59
60

1
2
3 (65) Zhang, M.; Cheng, J.; Xuan, X.; Zhou, J.; Cen, K. CO₂ Synergistic Reduction in a
4 Photoanode-Driven Photoelectrochemical Cell with a Pt-Modified TiO₂ Nanotube
5 Photoanode and a Pt Reduced Graphene Oxide Electrode. *ACS Sustain. Chem. Eng.*
6
7
8
9
10 **2016**, 4, 6344-6354, 10.1021/acssuschemeng.6b00909.

11
12 (66) Huang, X.; Shen, Q.; Liu, J.; Yang, N.; Zhao, G. CO₂ adsorption-enhanced
13 semiconductor/metal-complex hybrid photoelectrocatalytic interface for efficient formate
14 production. *Energy Environ. Sci.* **2016**, 9, 3161-3171, 10.1039/C6EE00968A.

15
16
17 (67) Kutz, R. B.; Chen, Q.; Yang, H.; Sajjad, S. D.; Liu, Z.; Masel, I. R. Sustainion
18 Imidazolium-Functionalized Polymers for Carbon Dioxide Electrolysis. *Energy Technol.*
19
20
21
22
23 **2017**, 5, 929-936, 10.1002/ente.201600636.

24
25 (68) Li, Y. C.; Zhou, D.; Yan, Z.; Gonçalves, R. H.; Salvatore, D. A.; Berlinguette, C. P.;
26 Mallouk, T. E. Electrolysis of CO₂ to Syngas in Bipolar Membrane-Based
27 Electrochemical Cells. *ACS Energy Lett.* **2016**, 1, 1149-1153,
28
29
30
31
32
33
34 10.1021/acsenerylett.6b00475.

35 (69) Zhou, X.; Liu, R.; Sun, K.; Chen, Y.; Verlage, E.; Francis, S. A.; Lewis, N. S.; Xiang,
36 C. Solar-Driven Reduction of 1 atm of CO₂ to Formate at 10% Energy-Conversion
37 Efficiency by Use of a TiO₂-Protected III–V Tandem Photoanode in Conjunction with a
38 Bipolar Membrane and a Pd/C Cathode. *ACS Energy Lett.* **2016**, 1, 764-770,
39
40
41
42
43
44
45 10.1021/acsenerylett.6b00317.

46 (70) Albo, J.; Sáez, A.; Solla-Gullón, J.; Montiel, V.; Irabien, A. Production of methanol
47 from CO₂ electroreduction at Cu₂O and Cu₂O/ZnO-based electrodes in aqueous solution.
48
49
50
51
52
53 *Appl. Catal., B* **2015**, 176-177, 709-717, 10.1016/j.apcatb.2015.04.055.

54 (71) Albo, J.; Vallejo, D.; Beobide, G.; Castillo, O.; Castaño, P.; Irabien, A. Copper-
55 Based Metal–Organic Porous Materials for CO₂ Electrocatalytic Reduction to Alcohols.
56
57
58
59
60 *Chem. Sus. Chem.* **2016**, 9, 1-11, 10.1002/cssc.201600693.

- 1
2
3 (72) Endrodi, B.; Bencsik, G.; Darvas, F.; Jones, R.; Rajeshwar, K.; Janáky, C.
4
5 Continuous-flow electroreduction of carbon dioxide. *Prog. Energy Combust. Sci.* **2017**,
6
7 62, 133-154, 10.1016/j.pecs.2017.05.005.
8
9
10 (73) Homayoni, H.; Chanmanee, W.; Tacconi, R.; Dennis, H.; Rajeshwar, K. Continuous
11
12 Flow Photoelectrochemical Reactor for Solar Conversion of Carbon Dioxide to Alcohols.
13
14 *J. Electrochem. Soc.* **2015**, 162 (8), 115-122, 10.1149/2.0331508jes.
15
16
17 (74) Xia, S.; Meng, Y.; Zhou, X.; Xue, J.; Pan, G.; Ni, Z. Ti/ZnO–Fe₂O₃ composite:
18
19 Synthesis, characterization and application as a highly efficient photoelectrocatalyst for
20
21 methanol from CO₂ reduction. *Appl. Catal., B* **2016**, 187, 122-133,
22
23 10.1016/j.apcatb.2016.01.027.
24
25
26 (75) Wood, J.; Summers, H.; Clark, A.; Kaeffer, N.; Braeutigam, M.; Carbone, L.;
27
28 D’Amario, L.; Fan, K.; Farre, Y.; Narbey, S.; Oswald, F.; Stevens, A.; Parmenter, D.J.;
29
30 Fay, W.; La Torre, A. A comprehensive comparison of dye-sensitized NiO photocathodes
31
32 for solar energy conversion. *Phys. Chem. Chem. Phys* **2016**, 18, 10727-10738,
33
34 10.1039/C5CP05326A.
35
36
37 (76) Qin, G.; Zhang, Y.; Keb, X.; Tong, X.; Sun, Z.; Liang, M.; Xue, S. Photocatalytic
38
39 reduction of carbon dioxide to formic acid, formaldehyde, and methanol using dye-
40
41 sensitized TiO₂ film. *Appl. Catal., B* **2013**, 129, 599-605, 10.1016/j.apcatb.2012.10.012.
42
43
44 (77) Kaneco, S.; Katsumata, H.; Suzuki, T.; Ohta, K. Photoelectrocatalytic reduction of
45
46 CO₂ in LiOH/methanol at metal-modified p-InP electrodes. *Appl. Catal. B* **2006**, 64, 139-
47
48 145, 10.1016/j.apcatb.2005.11.012.
49
50
51 (78) Cheng, J.; Zhang, M.; Liu, J.; Zhou, J.; Cen, K. Cu foam cathode used as Pt-RGO
52
53 catalyst matrix to improve CO₂ reduction in a photoelectrocatalytic cell with TiO₂
54
55 photoanode. *J. Mater. Chem. A* **2015**, 3, 12947-12957, 10.1039/C5TA03026A.
56
57
58
59
60

- 1
2
3 (79) Chang, X.; Wang, T.; Zhang, P.; Wei, Y.; Zhao, J.; Gong, J. Stable Aqueous
4 Photoelectrochemical CO₂ Reduction by a Cu₂O Dark Cathode with Improved Selectivity
5 for Carbonaceous Products. *Angew. Chem. Int. Ed.* **2016**, *55*, 1-6,
6 10.1002/anie.201602973.
7
8
9
10
11 (80) La Tempa, T. J.; Rani, S.; Bao, N.; Grimes, C.A. Generation of fuel from CO₂
12 saturated liquids using a p-Si nanowire // n-TiO₂ nanotube array photoelectrochemical
13 cell. *Nanoscale* **2012**, *4*, 2245-2250, 10.1039/c2nr00052k.
14
15
16
17 (81) Jacobsson, T. J.; Fjällström, V.; Edoffb, M.; Edvinsson, T.. Sustainable solar
18 hydrogen production: from photoelectrochemical cells to PV-electrolyzers and back
19 again. *Energy Environ. Sci.*, **2014**, *7*, 2056, 10.1039/C4EE00754A.
20
21
22
23 (82) Asadi, M.; Kim, K.; Liu, C.; Addepalli, A. V.; Abbasi, P.; Yasaei, P.; Phillips, P.;
24 Behranginia, A.; Cerrato, J. M.; Haasch, R.; Zapol, P.; Kumar, B.; Klie, R. F.; Abiade, J.;
25 Curtiss, L. A.; Salehi-Khojin, A.. Nanostructured transition metal dichalcogenide
26 electrocatalysts for CO₂ reduction in ionic liquid. *Science* **2016**, *353*, 467-470,
27 10.1126/science.aaf4767.
28
29
30
31 (83) White, J. L.; Herb, J. T.; Kaczur, J. J.; Majsztzik, P. W.; Bocarsly, A. B. Photons to
32 formate: Efficient electrochemical solar energy conversion via reduction of carbon
33 dioxide. *J. CO₂ Util.* **2014**, *7*, 1-5, 10.1016/j.jcou.2014.05.002.
34
35
36
37 (84) Li, K.; Ana, X.; Parka, K.H.; Khraishehb, M.; Tanga, J. A critical review of CO₂
38 photoconversion: Catalysts and reactors. *Catal. Today* **2014**, *224*, 3-12,
39 10.1016/j.cattod.2013.12.006.
40
41
42
43 (85) Inoue, T.; Fujishima, A.; Konishi, S.; Honda, K. Photoelectrocatalytic reduction of
44 carbon dioxide in aqueous suspensions of semiconductor powders. *Nature* **1979**, *277*,
45 637-638, 10.1038/277637a0.
46
47
48
49
50
51
52
53
54
55
56
57
58
59
60

- 1
2
3 (86) Sekiya, T.; Ichimura, K.; Igarashi, M.; Kurita, S. Absorption spectra of anatase TiO₂
4 single crystals heat-treated under oxygen atmosphere. *J. Phys. Chem. Solids* **2000**, 61,
5 1237-1242, 10.1016/S0022-3697(99)00424-2.
6
7
8
9
10 (87) Liu, L.; Zhao, H.; Andino, J.M.; Li, Y. Photocatalytic CO₂ Reduction with H₂O on
11 TiO₂ Nanocrystals: Comparison of Anatase, Rutile, and Brookite Polymorphs and
12 Exploration of Surface Chemistry. *ACS Catal.* **2012**, 2(8), 1817-1828,
13 10.1021/cs300273q.
14
15
16
17
18 (88) Wang, T.; Meng, X.; Li, P.; Ouyang, S.; Chang, K.; Liu, G.; Meia, Z.; Ye, J.
19 Photoreduction of CO₂ over the well-crystallized ordered mesoporous TiO₂ with the
20 confined space effect. *Nano Energy* **2014**, 9, 50-60, 10.1016/j.nanoen.2014.06.027.
21
22
23
24
25 (89) Zhao, H.; Pan, F.; Li, Y. A review on the effects of TiO₂ surface point defects on
26 CO₂ photoreduction with H₂O. *J Materiomics* **2017**, 3, 17-32,
27 10.1016/j.jmat.2016.12.001.
28
29
30
31
32 (90) Barton, E.; Rampulla, M.; Bocarsly, B. Selective Solar-Driven Reduction of CO₂ to
33 Methanol Using a Catalyzed *p*-GaP Based Photoelectrochemical Cell. *J. Am. Chem. Soc.*
34 **2008**, 130, 6342-6344, 10.1021/ja0776327.
35
36
37
38
39 (91) Yu, Y.; Zhang, Z.; Yin, X.; Kvit, A.; Liao, Q.; Kang, Z.; Yan, X.; Zhang, Y.; Wang,
40 X. Enhanced photoelectrochemical efficiency and stability using a conformal TiO₂ film
41 on a black silicon photoanode. *Nature Energy* **2017**, 156-157, 134-140,
42 10.1038/nenergy.2017.45.
43
44
45
46
47 (92) Magesh, G.; Kim, E.S.; Kang, H.J.; Banu, M.; Kim, J.Y.; Kim, J.H.; Lee, J.S. A
48 versatile photoanode-driven photoelectrochemical system for conversion of CO₂ to fuels
49 with high faradaic efficiencies at low bias potentials. *J. Mater. Chem. A* **2014**, 2, 2044-
50 2049, 10.1039/C3TA14408A.
51
52
53
54
55
56
57
58
59
60

1
2
3 (93) Song, J. T.; Ryoo, H.; Cho, M.; Kim, J.; Kim, J. G.; Chung, S. Y.; Oh, J. Nanoporous
4 Au Thin Films on Si Photoelectrodes for Selective and Efficient Photoelectrochemical
5 CO₂ Reduction. *Adv. Energy Mater.* **2017**, 7, 1601103, 10.1002/aenm.201601103.
6
7

8
9
10 (94) Morikawa, T.; Sato, S.; Arai, T.; Uemura, K.; Yamanaka, K.I.; Suzuki, T.M.; Kajino,
11 T.; Motohiro, T. Selective CO₂ Reduction Conjugated with H₂O Oxidation Utilizing
12 Semiconductor/Metal-Complex Hybrid Photocatalysts. *AIP Conference Proceedings*
13 **2013**, 1568:1, 11-15, 10.1021/ja204881d.
14
15

16
17 (95) Sahara, G.; Kumagai, H.; Maeda, K.; Kaeffer, N.; Artero, V.; Higashi, M., Abe, R.;
18 Ishitani, O. Photoelectrochemical Reduction of CO₂ Coupled to Water Oxidation Using
19 a Photocathode With a Ru(II)–Re(I) Complex Photocatalyst and a CoO_x/TaON
20 Photoanode. *J. Am. Chem. Soc.* **2016**, 138, 14152-14158, 10.1021/jacs.6b09212.
21
22

23
24 (96) Hu, B.; Guild, C.; Suib, S.L. Thermal, electrochemical, and photochemical
25 conversion of CO₂ to fuels and value-added products. *J. CO₂ Util.* **2013**, 1, 18-27,
26 10.1016/j.jcou.2013.03.004.
27
28

29
30 (97) Petit J.P.; Chartier, P.; Beley, M.; Deville, J.P. Molecular catalysts in
31 photoelectrochemical cells Study of an efficient system for the selective
32 photoelectroreduction of CO₂: *p*-GaI or *p*-GaAs / Ni(cyclam)²⁺, aqueous medium. *J.*
33 *Electroanal. Chem.*, **1989**, 269, 267-281, 10.1016/0022-0728(89)85137-X.
34
35

36
37 (98) Hirota, K.; Tryk, A.; Yamamoto, T.; Hashimoto, K.; Okawa, M.; Fujishima, A.
38 Photoelectrochemical reduction of CO₂ in a high-pressure CO₂ + methanol medium at *p*-
39 type semiconductor electrodes. *J. Phys. Chem. B* **1998**, 102, 9834-9843,
40 10.1021/jp9822945.
41
42

43
44 (99) Kumar, B.; Smieja, J.M.; Kubiak, C.P. Photoreduction of CO₂ on *p*-type Silicon
45 Using Re(bipy-But)(CO)₃Cl: Photovoltages Exceeding 600 mV for the Selective
46 Reduction of CO₂ to CO. *J. Phys. Chem. C* **2010**, 114, 14220-14223, 10.1021/jp105171b.
47
48
49
50
51
52
53
54
55
56
57
58
59
60

- 1
2
3 (100) Yang, K.D.; Ha, Y.; Sim, U.; An, J.; Lee, C.W.; Jin, K.; Kim, Y.; Park, J.; Hong,
4 J.S.; Lee, J.H.; Lee, H-E.; Jeong, H.-Y.; Kim, H.; Nam, K.T. Graphene Quantum Sheet
5 Catalyzed Silicon Photocathode for Selective CO₂ Conversion to CO. *Adv. Funct. Mater.*
6 **2016**, 26, 233-242, 10.1002/adfm.201502751.
7
8
9
10
11 (101) Kaneco, S.; Katsumata, H.; Suzuki, T.; Ohta, K. Photoelectrochemical reduction of
12 carbon dioxide at p-type gallium arsenide and p-type indium phosphide electrodes in
13 methanol. *Chem. Eng. J.* **2006**, 116, 227-231, 10.1016/j.cej.2005.12.014.
14
15
16
17 (102) Lin, X.; Gao, Y.; Jiang, M.; Zhang, Y.; Hou, Y.; Dai, W.; Wang, S.; Ding, Z.
18 Photocatalytic CO₂ reduction promoted by uniform perovskite hydroxide CoSn(OH)₆
19 nanocubes. *Appl. Catal., B* **2018**, 224, 1009-1016, 10.1016/j.apcatb.2017.11.035.
20
21
22
23 (103) Sahara, G.; Abe, R.; Higashi, M.; Morikawa, T.; Maeda, K.; Ueda, Y.; Ishitani, O.
24 Photoelectrochemical CO₂ reduction using a Ru(II)-Re(I) multinuclear metal complex on
25 a p-type semiconducting NiO electrode. *Chem. Commun.* **2015**, 51, 10722-10725,
26 10.1039/C5CC02403J.
27
28
29
30 (104) Kaneco, S.; Ueno, Y.; Katsumata, H.; Suzuki, T.; Ohta, K. Photoelectrochemical
31 reduction of CO₂ at p-InP electrode in copper particle-suspended methanol. *Chem. Eng.*
32 *J.* **2009**, 148, 57-62, 10.1016/j.cej.2008.07.038.
33
34
35 (105) Song, J.; Ryoo, H.; Cho, M.; Kim, J.; Kim, J.G.; Chung, S.; Oh, J. Nanoporous Au
36 Thin Films on Si Photoelectrodes for Selective and Efficient Photoelectrochemical CO₂
37 Reduction. *Adv. Energy Mater.* **2016**, 1601103, 10.1002/aenm.201601103.
38
39
40
41 (106) Weng, B.; Wei, W.; Yiliguma; Wu, H.; Alenizi, A.M.; Zheng, G. Bifunctional CoP
42 and CoN Porous Nanocatalysts Derived from ZIF-67 In Situ Grown on Nanowire
43 Photoelectrodes for Efficient Photoelectrochemical Water Splitting and CO₂ Reduction.
44 *J. Mater. Chem. A* **2016**, 4, 15353-1536, 10.1039/C6TA06841C.
45
46
47
48
49
50
51
52
53
54
55
56
57
58
59
60

- 1
2
3 (107) Jiang, M.; Wu, H.; Li, Z.; Ji, D.; Li, W.; Liu, Y., Yuan, D.; Wang, B.; Zhang, Z.
4
5 Highly selective photoelectrochemical conversion of carbon dioxide to formic acid. ACS
6
7 Sustainable Chem. Eng. **2018**, 6(1), 82-87, 10.1021/acssuschemeng.7b03272.
8
9
10 (108) Gu, J.; Wuttig, A.; Krizan, J.W.; Hu, Y.; Detweiler, Z.M.; Cava, R.J.; Bocarsly,
11
12 A.B. Mg-Doped CuFeO₂ Photocathodes for Photoelectrochemical Reduction of Carbon
13
14 Dioxide. J. Phys. Chem. C **2013**, 117, 12415-12422, 10.1021/jp402007z.
15
16
17 (109) Shen, Q.; Chen, Z.; Xiaofeng, H.; Liu, M.; Zhao, G. High-yield and Selective
18
19 Photoelectrocatalytic Reduction of CO₂ to Formate by Metallic Copper Decorated Co₃O₄
20
21 Nanotube Arrays. Environ. Sci. Technol. **2015**, 49, 5828-5835, 10.1021/acs.est.5b00066.
22
23
24 (110) Irtem, E.; Hernández-Alonso, M.D.; Parra, A.; Fàbrega, C.; Penelas-Pérez, G.;
25
26 Morante, J.R.; Andreu, T. A photoelectrochemical flow cell design for the efficient CO₂
27
28 conversion to fuels. Electrochim. Acta **2017**, 240, 225-230,
29
30 10.1016/j.electacta.2017.04.072.
31
32
33 (111) Irtem, E.; Andreu, T.; Parra, A.; Hernandez-Alonso, M.D.; García-Rodríguez, S.;
34
35 Riesco-García, J.M.; Penelas-Pérez, G.; Morante, J.R.. Low-energy formate production
36
37 from CO₂ electroreduction using electrodeposited tin on GDE. J. Mater. Chem. A, **2016**,
38
39 4, 13582-13588, 10.1039/C6TA04432H.
40
41
42 (112) Arai, T.; Sato, S.; Uemura, K.; Morikawa, T.; Kajino, T.; Motohiro, T.
43
44 Photoelectrochemical reduction of CO₂ in water under visible-light irradiation by a *p*-
45
46 type InP photocathode modified with an electropolymerized ruthenium complex. Chem.
47
48 Commun. **2010**, 46, 6944-6946, 10.1039/C0CC02061C.
49
50
51 (113) Arai, T.; Tajima, S.; Sato, S.; Uemura, K.; Morikawa, T.; Kajino, T. Selective CO₂
52
53 conversion to formate in water using a CZTS photocathode modified with a ruthenium
54
55 complex polymer. Chem. Commun. **2011**, 47, 12664-12666, 10.1039/C1CC16160A.
56
57
58
59
60

- 1
2
3 (114) Zhang, M.; Cheng, J.; Xuan, X.; Zhou, J.; Cen, K. Pt/graphene aerogel deposited in
4 Cu foam as a 3D binder-free cathode for CO₂ reduction into liquid chemicals in a TiO₂
5 photoanode-driven photoelectrochemical cell. *Chem. Eng. J.* **2017**, 322, 22-32,
6 10.1016/j.cej.2017.03.126.
7
8 (115) Ferreira de Brito, J.; Alves da Silva, A.; Cavaleiro, A.J.; Zaroni, M.V.B.
9 Evaluation of the Parameters Affecting the Photoelectrocatalytic Reduction of CO₂ to
10 CH₃OH at Cu/Cu₂O Electrode. *Int. J. Electrochem. Sci.* **2014**, 9, 5961-5973.
11
12 (116) Li, P.; Xu, J.; Jing, H.; Wu, C.; Peng, H.; Lu, J.; Yin, H. Wedged N-doped CuO
13 with more negative conductive band and lower over potential for high efficiency
14 photoelectric converting CO₂ to methanol. *Appl. Catal., B* **2014**, 156-157, 134-140,
15 10.1016/j.apcatb.2014.03.011.
16
17 (117) Ferreira de Brito, J.; Araujo, A.R.; Rajeshwar, K.; Zaroni, M.V.B.
18 Photoelectrochemical reduction of CO₂ on Cu/Cu₂O films: Product distribution and pH
19 effects. *Chem. Eng. J.* **2015**, 264, 302-309, 10.1016/j.cej.2014.11.081.
20
21 (118) Ganesh, I. Conversion of carbon dioxide into methanol – a potential liquid fuel:
22 Fundamental challenges and opportunities (a review). *Renew. Sustain. Energy Rev.* **2014**,
23 31, 221-257, 10.1016/j.rser.2013.11.045.
24
25 (119) Yuan, J.; Wang, X.; Gu, C.; Sun, J.; Ding, W.; Wei, J.; Zuo X.; Hao. C.
26 Photoelectrocatalytic reduction of carbon dioxide to methanol at cuprous oxide foam
27 cathode. *RSC Adv.* **2017**, 7, 24933-24939, 10.1039/C7RA03347H.
28
29 (120) Lee, K.; Lee, S.; Cho, H.; Jeong, S.; Kim, W.D.; Lee, S.; Lee, D.C. Cu⁺ -
30 incorporated TiO₂ overlayer on Cu₂O nanowire photocathodes for enhanced
31 photoelectrochemical conversion of CO₂ to methanol. *J. Energy Chem.* **2018**, 27, 264-
32 270, 10.1016/j.jechem.2017.04.019.
33
34
35
36
37
38
39
40
41
42
43
44
45
46
47
48
49
50
51
52
53
54
55
56
57
58
59
60

- 1
2
3 (121) Yang, Z.; Wang, H.; Song, W.; Wei, W.; Mu, Q.; Kong, B.; Li, P.; Yin, H. One
4 dimensional SnO₂ NRs/Fe₂O₃ NTs with dual synergistic effects for photoelectrocatalytic
5 reduction CO₂ into methanol. *J. Colloid Interface Sci.* **2017**, 486, 232-240,
6 10.1016/j.jcis.2016.09.055.
7
8
9
10
11 (122) Wei, W.; Yang, Z.; Song, W.; Hu, F.; Luan, B.; Li, P.; Yin, H. Different CdSeTe
12 structure determined photoelectrocatalytic reduction performance for carbon dioxide. *J.*
13 *Colloid Interface Sci.* **2017**, 496, 327-333, 10.1016/j.jcis.2016.11.054.
14
15
16
17 (123) Thompson, J. F.; Chen, B.; Kubo, M.; Londoño, N.; Minuzzo, J. Artificial
18 photosynthesis device development for CO₂ photoelectrochemical conversion. *MRS Adv.*
19 **2016**, 1, 447-452, 10.1557/adv.2016.111.
20
21
22
23 (124) Ampelli, C.; Passalacqua, R.; Genovese, C.; Perathoner, S.; Centi, G. A Novel
24 Photo-electrochemical Approach for the Chemical Recycling of Carbon Dioxide to Fuels.
25 *Chem. Eng. Trans.* **2011**, 25, 683-688, 10.3303/CET1125114.
26
27
28
29 (125) Yuan, J.; Xiao, B.; Hao, C. Photoelectrochemical Reduction of Carbon Dioxide to
30 Ethanol at Cu₂O Foam Cathode. *Int. J. Electrochem. Sci.* **2017**, 12, 8288-8294,
31 10.20964/2017.09.36.
32
33
34
35 (126) Qi, Y.; Xu, Q.; Wang, Y.; Yan, B.; Ren, Y.; Chen, Z. CO₂-Induced Phase
36 Engineering: Protocol for Enhanced Photoelectrocatalytic Performance of 2D MoS₂
37 Nanosheets. *ACS Nano* **2016**, 10, 2903-2909, 10.1021/acsnano.6b00001.
38
39
40 (127) Kong, Q.; Kim, D.; Liu, C.; Yu, Y.; Su, Y.; Li, Y.; Yang, P. Directed Assembly of
41 Nanoparticle Catalysts on Nanowire Photoelectrodes for Photoelectrochemical CO₂
42 Reduction. *Nano Lett.* **2016**, 16, 5675-5680, 10.1021/acs.nanolett.6b02321.
43
44
45
46 (128) Cheng, J.; Zhang, M.; Wu, G.; Wang, X.; Zhou, J.; Cen, K. Optimizing CO₂
47 reduction conditions to increase carbon atom conversion using a Pt-RGO||Pt TNT
48
49
50
51
52
53
54
55
56
57
58
59
60

1
2
3 photoelectrochemical cell. *Sol. Energy Mater. Sol. Cells* **2015**, 132, 606-614,
4
5 10.1016/j.solmat.2014.10.015.

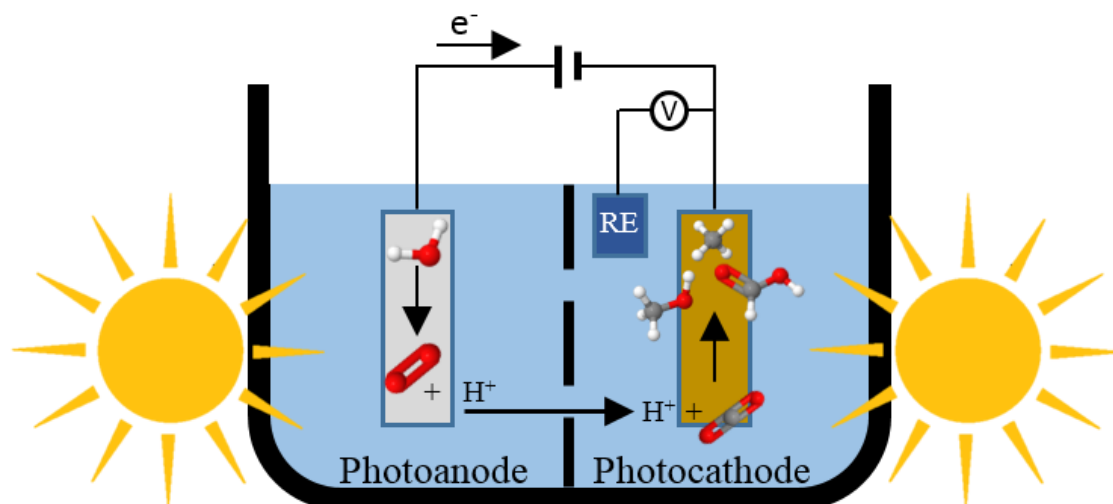
6
7 (129) Hasan, M.R.; Hamid, S.B.A.; Basirun, W.J.; Suhaimy, S.H.M.; Mat, A.N.C. A sol-
8 gel derived, copper-doped, titanium dioxide-reduced graphene oxide nanocomposite
9 electrode for the photoelectrocatalytic reduction of CO₂ to methanol and formic acid. *RSC*
10 *Advances* **2015**, 5, 77803-77813, 10.1039/C5RA12525A.

11
12 (130) Jang, Y. J.; Jeong, I.; Lee, J.; Lee, J.; Ko, M. J.; Lee, J. S.. Unbiased sunlight-driven
13 artificial photosynthesis of carbon monoxide from CO₂ using a ZnTe-based photocathode
14 and a perovskite solar cell in tandem. *ACS Nano* **2016**, 10, 6980-6987,
15 10.1021/acsnano.6b02965.

16
17 (131) Wang, Y.; Fan, S.; AlOtaibi, B.; Wang, Y.; Li, L.; Mi, Z. A monolithically
18 integrated gallium nitride nanowire/silicon solar cell photocathode for selective carbon
19 dioxide reduction to methane. *Chem. Eur. J.* **2016**, 22, 8809-8813,
20 10.1002/chem.201601642.

21
22 (132) Nath, N. C. D.; Choi, S. Y.; Jeong, H. W.; Lee, J. J.; Park, H.. Stand-alone
23 photoconversion of carbon dioxide on copper oxide wire arrays powered by tungsten
24 trioxide/dye-sensitized solar cell dual absorbers. *Nano Energy* **2016**, 25, 51-59,
25 10.1016/j.nanoen.2016.04.025.

26
27
28
29
30
31
32
33
34
35
36
37
38
39
40
41
42
43
44
45
46
47
48
49 **Table of Contents**
50
51
52
53
54
55
56
57
58
59
60



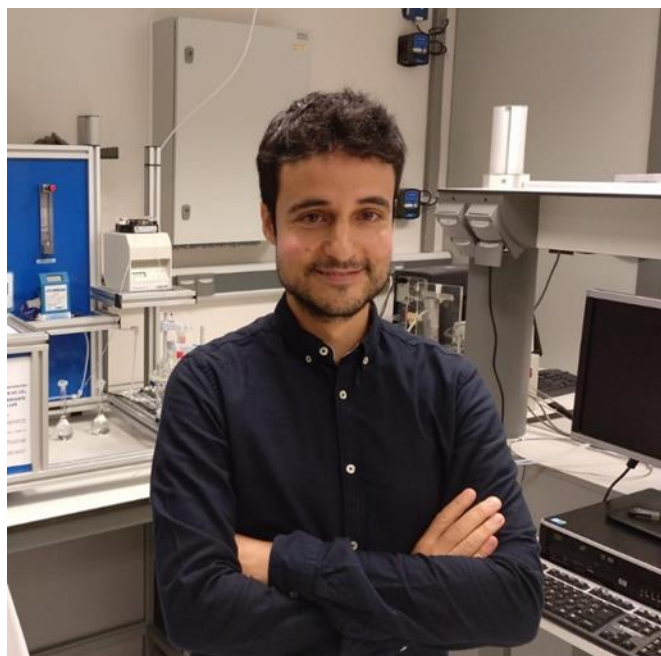
23
24
25
26
27
28
29
30
31
32
33
34
35
36
37
38
39
40
41
42
43
44
45
46
47
48
49
50
51
52
53
54
55
56
57
58
59
60

The PEC technology presents potential for an enhanced CO₂ reduction efficiency under the sun allowing the production of the electrons required and the oxidation/reduction reactions at the same device.

AUTHOR INFORMATION

Sergio Castro studied Chemical Engineering at University of Cantabria (2015), where he obtained his Master's (2017) in Chemical Engineering. At present, he is a Predoctoral Researcher in the Department of Chemical and Biomolecular Engineering and member of the DePRO research group headed by Prof. Irabien (<http://grupos.unican.es/depro/>) in the same university. The primary focus of his research areas are in the field of the electro- and

photoelectrocatalytic conversion of CO₂ into valuable products.



Jonathan Albo obtained his MSc in Chemical Engineering (2010) from the University of Cantabria. In 2012, he completed his PhD in Chemical Engineering at the same University, focused on the development of new membrane-based processes for CO₂ separation. He next held a JSPS

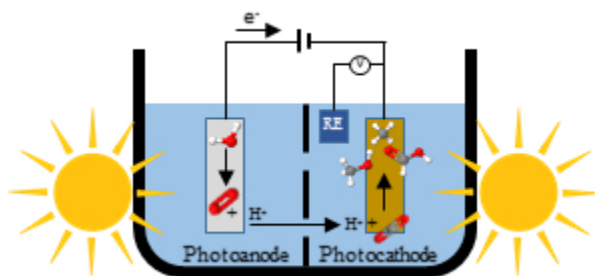
postdoctoral fellowship (2013) at Hiroshima University and then joined the University of the Basque Country as a Juan de la Cierva researcher (2014-2016). At present, he is Ramón y Cajal senior researcher at the Chemical and Biomolecular Engineering

1
2
3 Department, University of Cantabria. His main research interests are in the field of
4
5 electro-photoelectro-and-photo-catalytic conversion of CO₂ to value-added chemicals.
6
7



Angel Irabien is Full Professor of Chemical Engineering in the Department of Chemical and Biomolecular Engineering at the University of Cantabria (Spain) after his PhD thesis, Associated Professor position in the Basque Country University and Academic Visitor stays in the Kings College (U London, UK), Friedrich Alexander Universität (Germany) and Oxford University (UK). His research interest include the development of carbon capture and utilization processes based on electrochemical reactors and renewable energy and the application of Life

35
36 Cycle Thinking to the Chemical and Process Engineering.
37
38
39
40
41
42
43
44
45
46
47
48
49
50
51
52
53
54
55
56
57
58
59
60



82x44mm (96 x 96 DPI)